Measurements and Validation for the Twelve Month Particulate Matter Study in Hong Kong

Final Report

PREPARED BY:

Dr. Judith C. Chow
Dr. John G. Watson
Mr. Steven D. Kohl
Mr. Matt P. Gonzi
Dr. L.-W. Antony Chen

DESERT RESEARCH INSTITUTE
2215 Raggio Parkway
Reno, NV 89512
USA

PREPARED FOR:

Environmental Protection Department
The Government of Hong Kong Special Administrative Region
33/F, Revenue Tower
5 Gloucester Rd.
Wan Chai
Hong Kong

December 12, 2002

Measurements and Validation for the Twelve Month Particulate Matter Study in Hong Kong

Final Report

PREPARED BY:

Dr. Judith C. Chow
Dr. John G. Watson
Mr. Steven D. Kohl
Mr. Matt P. Gonzi
Dr. L.-W. Antony Chen

DESERT RESEARCH INSTITUTE
2215 Raggio Parkway
Reno, NV 89512
USA

PREPARED FOR:

Environmental Protection Department
The Government of Hong Kong Special Administrative Region
33/F, Revenue Tower
5 Gloucester Rd.
Wan Chai
Hong Kong

December 12, 2002

TABLE OF CONTENTS

LIST OF FIGURES

LIST OF TABLES

1. INTRODUCTION

1.1 Study Objectives

The Desert Research Institute (DRI) assisted the Hong Kong Environmental Protection Department (HKEPD) with sampling support and analysis of $PM_{2.5}$ samples acquired over the course of one year from 11/06/00 to 10/26/01. The objectives of this study were to:

- Evaluate sampling and measurement methods for inorganic and organic particulate components and for gaseous precursors and end-products of particle-forming atmospheric reactions.

- Determine the organic and inorganic composition of $PM_{2.5}$ and how it differs by season and proximity to different source types.

- Based on ambient concentrations of marker compounds, source measurements performed elsewhere, and available Hong Kong emissions inventories, determine which sources are the most probable contributors to $PM_{2.5}$ in Hong Kong.

Prior to the start of the study, DRI was contracted to provide technical support and planning for sampling setup and strategy. These objectives included:

- Review documents, reports, papers, and data sets pertaining to $PM_{2.5}$ and soluble organic species in the study area.

- Provide technical advice regarding project design, site selection, sampling methodology, filter weighing, analytical methodology, data interpretation, and QA/QC procedures for the study.

- Attend a kickoff meeting for the study in Hong Kong and accomplish the following tasks.
  - Comment on the overall $PM_{2.5}$ monitoring and sampling set up for the present project in Hong Kong.
  - Site visits to the three monitoring stations tentatively selected (Mong Kok, Tsuen Wan, and Hok Tsui).
  - Visit the EPD-designated laboratories.
  - Review vapor-phase toxic air pollutant (TAP) sampling methodology and analysis.

These tasks were accomplished, and the official sampling start date was 11/06/00.

1.2 Background

The Hong Kong Environmental Protection Department (HKEPD) currently has not established or adopted ambient air quality standards for fine particulate matter, particles with aerodynamic diameters less than 2.5 microns ($PM_{2.5}$). Current standards in Hong Kong reflect U.S. Environmental Protection Agency (EPA) National Ambient Air Quality Standards (NAAQS) for PM_{10}.

Chemically speciated $PM_{2.5}$ and PM_{10} data from a 1998-99 pilot at Tsuen Wan, Hong Kong, showed that: 1) ~70% of PM_{10} is in the $PM_{2.5}$ fraction, 2) carbonaceous aerosol and secondary ammonium sulfate constituted a major portion of $PM_{2.5}$, 3) $PM_{2.5}$ concentrations and compositions varied over twofold between the warm and cold seasons, and 4) elevated levels of organic carbon were the main contributor to elevated $PM_{2.5}$ concentrations during winter.

The main objective of this report is to document $PM_{2.5}$ measurements and data validation for the yearlong study. This data will be analyzed to characterize the composition and temporal and spatial variations of $PM_{2.5}$ concentrations.

1.3 Technical Approach

During the sampling period from 11/06/00 to 10/26/01, 24-hour $PM_{2.5}$ mass measurements were acquired every sixth day from the roadside-source-dominated Mong Kok (MK) site, the urban Tsuen Wan (TW) site, and the regional background Hok Tsui (HT) site. Two Partisol particle samplers (Rupprecht & Patashnick, Albany, NY) were used at each site to obtain $PM_{2.5}$ samples on both Teflon-membrane and quartz-fiber 47-mm filters. All sampled Teflon-membrane and quartz-fiber filters were analyzed for mass by gravimetry at HKEPD and then subjected to full chemical analysis at DRI as documented in Section 2.2.

1.4 Guide to Report

This section has stated the background and objectives of the Twelve Month Particulate Matter Study in Hong Kong. Section 2 documents the ambient monitoring network and the unified database compiled from these measurements. The ambient database is assembled, validated, and documented in Section 3. A report summary is provided in Section 4. The bibliography and references are assembled in Section 5.

2. SAMPLING NETWORK

2.1 Ambient Network

Twenty-four-hour $PM_{2.5}$ filter samples were taken at three sites in Hong Kong. Sampling took place every sixth day from 11/06/00 to 10/26/01. The ambient monitoring network shown in Figure 2-1 was designed to represent roadside (source), urban (receptor), and rural (background) areas that characterize $PM_{2.5}$ in Hong Kong. The sampling locations consisted of an urban roadside site at Mong Kok (MK), an urban site at Tsuen Wan (TW), and a rural regional background site at Hok Tsui (HT). Table 2-1 lists the site names, codes, locations, elevations, and a description of each site.

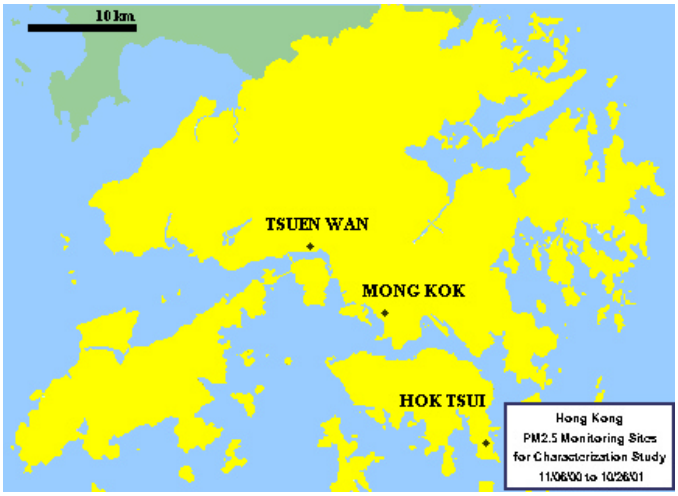

Figure 2-1. Map of the Hong Kong study area.

Table 2-1. Description of monitoring sites.

Site Name (Code) and Location	Elevation above Mean Sea Level (MSL)	Site Description
Mong Kok (MK) 4E Mong Kok Rd.	~17 m	An urban roadside site in southern Hong Kong with heavy traffic and restaurant cooking emissions nearby. Located 2 km west of Kowloon.
Tsuen Wan (TW) Princess Alexandra Community Centre, 60 Tai Ho Road	~25 m	An urban, densely populated, residential site with mixed commercial and industrial developments. Located northwest of the MK site.
Hok Tsui (HT) Rural location	60 m	A rural background/transport site located about 20 km southeast of the MK site.

2.2 Ambient Particulate Measurements

Two Rupprecht & Patashnick Partisol samplers were used at each site to acquire the ambient particulate air samples. The Partisol samplers were equipped with an Andersen SA-246 size-selective inlet/WINS impactor to sample $PM_{2.5}$ at a flow rate of 16.7 L/min. At this flow rate, a nominal volume of 24.1 m^3 of ambient air would be sampled over a 24-hour period. A vacuum pump drew ambient air through the inlet and down through the filter. The flow rate was controlled by a dry gas flow meter, downstream of the sample filter, and thus not affected by filter loading.

The Partisol samplers were configured to take either a Teflon-membrane filter or a quartz-fiber filter. Lippmann (1989), Lee and Ramamurthi (1993), Watson and Chow (1993, 1994), and Chow (1995) evaluated substrates for different sampling and analyses. Based on these evaluations, the filters chosen for this study were: 1) Pall Life Sciences (Ann Arbor, MI) polymethylpentane ringed, 2.0-µm pore size, 47-mm diameter, PTFE Teflon-membrane filters (#R2PJ047) for mass and elemental analysis; and 2) Pall Life Sciences (Ann Arbor, MI) 47-mm diameter, pre-fired quartz-fiber filters (#2500QAT-UP) for carbon and ion analyses.

As shown in Figure 2-2, the Teflon-membrane filter collected particles for mass analysis by gravimetry and elemental analysis (40 elements including Na, Mg, Al, Si, P, S, Cl, K, Ca, Ti, V, Cr, Mn, Fe, Co, Ni, Cu, Zn, Ga, As, Se, Br, Rb, Sr, Y, Zr, Mo, Pd, Ag, Cd, In, Sn, Sb, Ba, La, Au, Hg, Tl, Pb, and U) by x-ray fluorescence (Watson et al., 1999). The quartz-fiber filter, also a 47-mm diameter filter, was analyzed for mass by gravimetry, for chloride (Cl^-), nitrate (NO_3^-), and sulfate ($SO_4^=$) by ion chromatography (Chow and Watson, 1999), for ammonium (NH_4^+) by automated colorimetry, for water-soluble sodium (Na^+) and potassium (K^+) by atomic absorption spectrophotometry, and for carbon by two thermal evolution methods.

A major uncertainty in determining total carbon (TC) using thermal evolution methods results from differences in volatilization of certain organic compounds during sampling and storage (Fitz, 1990; Turpin et al., 1994; Chow et al., 1996). The split of organic and elemental carbon in thermal analysis, however, is even more ambiguous because it depends on temperature setpoints, temperature ramping rates, residence time at each setpoint, and combustion atmospheres, and these parameters are only empirically defined. At higher combustion temperatures, samples visibly darken as OC pyrolizes to EC in an oxygen-free environment. To overcome this problem, a laser is used to monitor changes in filter darkness during the thermal evolution process by detecting either filter reflectance (thermal/optical reflectance [TOR] method) or transmittance (thermal/optical transmittance [TOT] method).

Two analytical protocols, IMPROVE and STN, are used in thermal evolution analysis of TC, OC, and EC in the National Park Service's IMPROVE network and in USEPA's Speciation Trends Network (STN), respectively. In the IMPROVE protocol, total carbon is divided into eight carbon fractions as a function of temperature and oxidation environment (Chow et al., 1993b, 2001; Watson et al., 1994). The temperature in a pure helium (He)

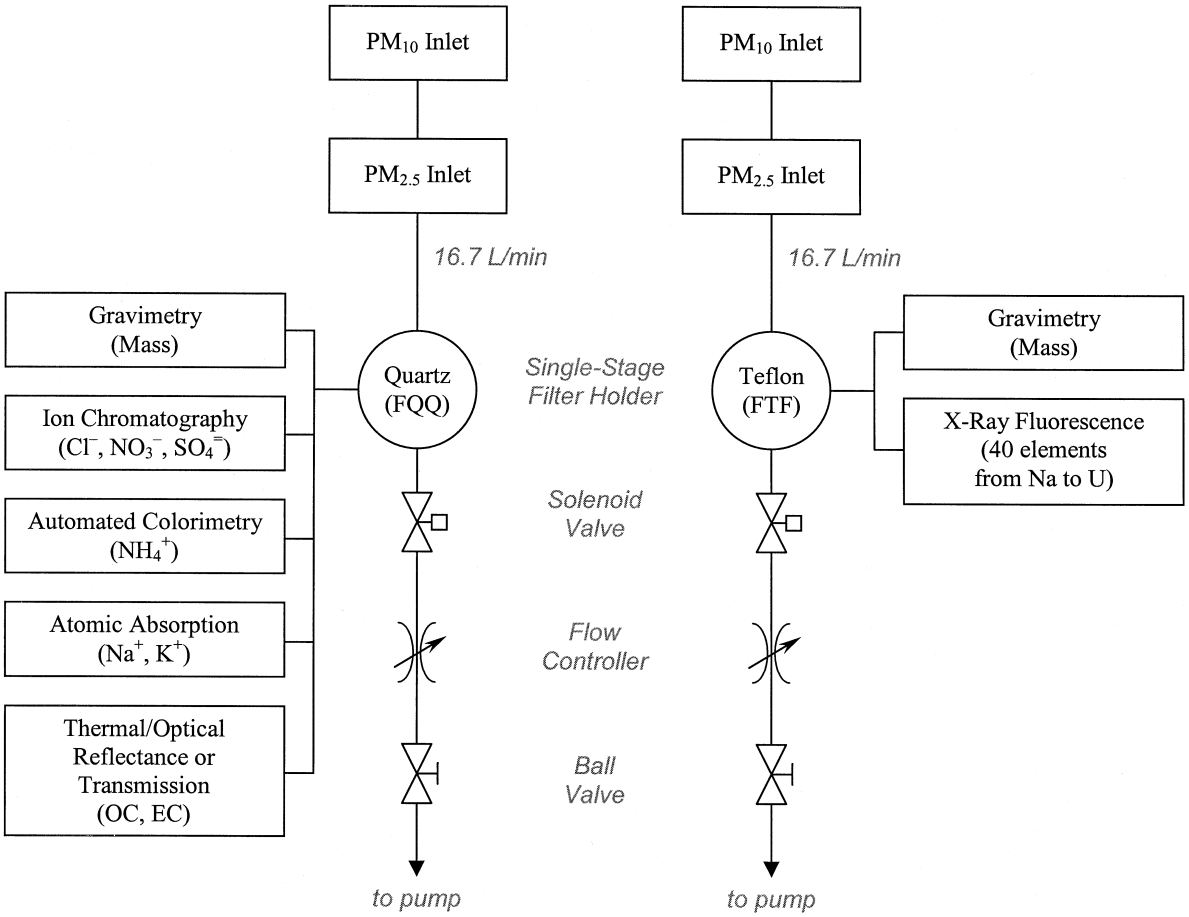

Figure 2-2. Schematic of $PM_{2.5}$ Partisol sampler configurations for the Twelve Month Particulate Matter Study in Hong Kong.

atmosphere ramps from 25 to 120 °C (OC1), from 120 to 250 °C (OC2), from 250 to 450 °C (OC3), and from 450 to 550 °C (OC4). Then, a 98% He/2% O_2 atmosphere is introduced and peaks are integrated at 550 °C (EC1), 700 °C (EC2), and 800 °C (EC3). The fraction of pyrolyzed organic carbon (OPR or OPT) is detected in the He/O_2 atmosphere at 550 °C prior to the return of reflectance or transmittance to its original value. In the IMPROVE protocol, OC is defined as OC1+OC2+OC3+OC4+OPR, and EC is defined as the difference between TC and OC.

The STN protocol is similar to the NIOSH protocol (NIOSH, 1996, 1998, 1999) except that temperature and combustion time are different for high-temperature carbon. A 900 °C OC4 fraction is determined in a pure He atmosphere in the STN protocol. Then the temperature is reduced to ~600 °C before a He/O_2 atmosphere is introduced. Besides the temperature protocol, another major difference between IMPROVE and STN is the residence time at each temperature setpoint. The IMPROVE protocol requires the FID signal to return to baseline before advancing to the next setpoint, but the combustion duration at each

setpoint is fixed in the STN protocol. Carbon fractions can be clearly separated in the IMPROVE protocol, but not in the STN protocol. The STN protocol is:

	Temperature (°C)	Duration Time (seconds)	Carrier Gas	Comment
Stage 0	----	10	He	Oven Purge
Stage 1	315	60	He	
Stage 2	480	60	He	
Stage 3	615	60	He	
Stage 4	900	90	He	
Stage 5	----	30	He	Cool oven
	----	10	He/O_2	
Stage 6	622	35	He/O_2	
Stage 7	675	45	He/O_2	
Stage 8	750	45	He/O_2	
Stage 9	825	45	He/O_2	
Stage 10	920	120	He/O_2	

In the STN protocol, OC and EC are defined differently under three possible scenarios.

- In the first scenario, laser transmittance returns to its initial value before the introduction of oxygen. No pyrolysis correction is applied (i.e., pyrolized OC [OPT] = 0). The OC/EC split is defined at the point where laser transmittance returns to its initial value. EC is defined as the difference between TC and OC. The STN protocol assumes this scenario.

- In the second scenario, laser transmittance returns to its initial value in the He/O_2 atmosphere (i.e., after the introduction of oxygen). OPT is defined as carbon evolving between the introduction of oxygen into the combustion atmosphere in stage 5 and laser transmittance returns to its initial value (i.e., OPT > 0). OC is defined as carbon evolving in stages 1, 2, 3, and 4, plus OPT. EC is defined as the difference between TC and OC. This scenario is similar to the IMPROVE TOR protocol.

- In the third scenario, laser transmittance returns to its initial value before the introduction of oxygen. No pyrolysis correction is applied (i.e., OPT = 0). The OC/EC split is defined at the point where oxygen is introduced. EC is defined as the difference between TC and OC (Chow et al., 2001).

In addition to IMPROVE TOR carbon data, this study reported two different versions of STN TOT carbon data: 1) OC/EC split determined when laser transmittance returns to its initial value regardless of when O_2 is added (STN TOT(i) = combination of first and second scenarios above); and 2) OC/EC split determined either when oxygen is introduced if OPT = 0, or when laser transmittance returns to its initial value if OPT > 0 (STN TOT(ii) = combination of second and third scenarios above).

The Partisol samplers were operated and maintained by ENSR Environmental International Ltd. throughout the study duration. The flow rate was periodically audited to

check for any flow discrepancies and to verify instrument performance. The Teflon-membrane and quartz-fiber filters were obtained prior to sampling by the HKEPD. The HKEPD was responsible for pre- and post- sampling procedures required for quality assurance and sample preservation. They were also responsible for conducting mass measurements and analysis on both filter types prior to shipping to DRI for chemical analysis.

3. DATABASE AND DATA VALIDATION

This section evaluates the precision, accuracy, and validity of the Hong Kong $PM_{2.5}$ filter data measurements. Numerous air quality studies have been conducted over the past decade, but the data obtained are often not available or applicable for data analysis and modeling because the databases lack documentation with regard to sampling and analysis methods, quality control/quality assurance procedures, accuracy specifications, precision calculations, and data validity. Lioy et al. (1980), Chow and Watson (1989), Watson and Chow (1992), and Chow and Watson (1994) summarize the requirements, limitations, and current availability of ambient and source databases in the United States. The Hong Kong $PM_{2.5}$ data set intends to meet these requirements. The data files for these studies have the following attributes:

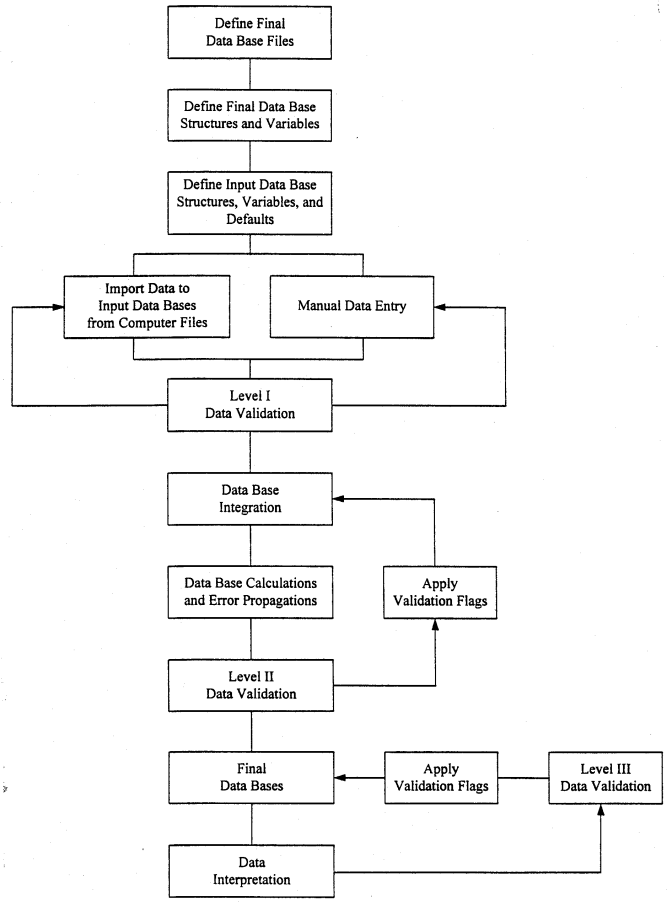

Figure 3-1. Flow diagram of the database management system.

- They contain the ambient observables needed to assess source/receptor relationships.
- They are available in a well-documented, computerized form accessible by personal computers and over the Internet.
- Measurement methods, locations, and schedules are documented.
- Precision and accuracy estimates are reported.
- Validation flags are assigned.

This section introduces the features, data structures, and contents of the Hong Kong $PM_{2.5}$ data archive. The approach that was followed to obtain the final data files is illustrated in Figure 3-1. Detailed data processing and data validation procedures are documented in Section 3.4. These data are available on floppy diskettes in Microsoft Excel (.xls) format for

convenient distribution to data users. The file extension identifies the file type according to the following definitions:

- TXT = ASCII text file
- DOC = Microsoft Word document
- XLS = Microsoft Excel spreadsheet

The assembled aerosol database for filter pack measurements taken during the study is fully described by the file "HKEPDFLDNAME.XLS" (see Table 3-1) which documents variable names, descriptions, and measurement units.

3.1 Database Structures and Features

The raw HKEPD data was processed with Microsoft FoxPro 2.6 for Windows (Microsoft Corp., 1994), a commercially available relational database management system. FoxPro can handle 256 fields of up to 4,000 characters per record and up to one billion records per file. This system can be implemented on most IBM PC-compatible desktop computers. The data base files (∗.DBF) can also be read directly into a variety of popular statistical, plotting, data base, and spreadsheet programs without having to use any specific conversion software. After processing, the final HKEPD data was converted from FoxPro to Microsoft Excel format for reporting ease and general use purposes.

In FoxPro, one of five field types (character, date, numerical, logical, or memo) was assigned to each observable. Sampling sites and particle size fractions are defined as "Character" fields, sampling dates are defined as "Date" fields, and measured data are defined as "Numeric" fields. "Logical" fields are used to represent a "yes" or "no" value applied to a variable, and "Memo" fields accommodate large blocks of textual information and are used to document the data validation results.

Data contained in different XBase files can be linked by indexing on and relating to common attributes in each file. Sampling site, sampling hour, sampling period, particle size, and sampling substrate IDs are, typically, the common fields among various data files that can be used to relate data in one file to the corresponding data in another file. To assemble the final data files, information was merged from many data files derived from field monitoring and laboratory analyses by relating information on the common fields cited above.

Table 3-1. Variable names, descriptions, and measurement units in the assembled aerosol database for filter pack measurements taken during the Twelve Month Particulate Matter Study in Hong Kong.

Field Code	Description	Measurement Unit
SITE	Sampling site	
DATE	Sampling date	
SIZE	particle size cut	µm
TSAMPLEID	HKEPD sample ID	
TFILTERID	HKEPD Teflon filter ID	
TID	DRI Teflon filter ID	
QSAMPLEID	HKEPD sample ID	
QFILTERID	HKEPD quartz filter ID	
QID	DRI quartz filter ID	
TFFLG	Teflon filter field flag (see FLDFLAGS.doc)	
QFFLG	Quartz filter field flag (see FLDFLAGS.doc)	
ANIF	Anion analysis flag (see CHEMFLAG.doc)	
N4CF	Ammonium analysis flag (see CHEMFLAG.doc)	
NAAF	Soluble sodium analysis flag (see CHEMFLAG.doc)	
KPAF	Soluble potassium analysis flag (see CHEMFLAG.doc)	
OETF	IMPROVE Carbon analysis flag (see CHEMFLAG.doc)	
STNOETF	STN Carbon analysis flag (see CHEMFLAG.doc)	
ELXF	XRF analysis flag (see CHEMFLAG.doc)	
TVOC	Teflon filter volume	m^3
TVOU	Teflon filter volume uncertainty (estimated at 5% of volume)	m^3
QVOC	Quartz filter volume	m^3
QVOU	Quartz filter volume uncertainty (estimated at 5% of volume)	m^3
MSGC	Teflon Mass concentration	$\mu g/m^3$
MSGU	Teflon Mass concentration uncertainty	$\mu g/m^3$
QMSGC	QMA Mass concentration	$\mu g/m^3$
QMSGU	QMA Mass concentration uncertainty	$\mu g/m^3$
CLIC	Chloride concentration	$\mu g/m^3$
CLIU	Chloride concentration uncertainty	$\mu g/m^3$
N3IC	Nitrate concentration	$\mu g/m^3$
N3IU	Nitrate concentration uncertainty	$\mu g/m^3$
S4IC	Sulfate concentration	$\mu g/m^3$
S4IU	Sulfate concentration uncertainty	$\mu g/m^3$
N4CC	Ammonium concentration	$\mu g/m^3$
N4CU	Ammonium concentration uncertainty	$\mu g/m^3$
NAAC	Soluble Sodium concentration	$\mu g/m^3$
NAAU	Soluble Sodium concentration uncertainty	$\mu g/m^3$
KPAC	Soluble Potassium concentration	$\mu g/m^3$
KPAU	Soluble Potassium concentration uncertainty	$\mu g/m^3$
O1TC	Organic Carbon Fraction 1concentration (IMPROVE Protocol)	$\mu g/m^3$
O1TU	Organic Carbon Fraction 1 concentration (IMPROVE Protocol) uncertainty	$\mu g/m^3$
O2TC	Organic Carbon Fraction 2 concentration (IMPROVE Protocol)	$\mu g/m^3$
O2TU	Organic Carbon Fraction 2 concentration (IMPROVE Protocol) uncertainty	$\mu g/m^3$
O3TC	Organic Carbon Fraction 3 concentration (IMPROVE Protocol)	$\mu g/m^3$
O3TU	Organic Carbon Fraction 3 concentration (IMPROVE Protocol) uncertainty	$\mu g/m^3$
O4TC	Organic Carbon Fraction 4 concentration (IMPROVE Protocol)	$\mu g/m^3$
O4TU	Organic Carbon Fraction 4 concentration (IMPROVE Protocol) uncertainty	$\mu g/m^3$

Table 3-1. (continued)

Field Code	Description	Measurement Unit
OPTC	Pyrolyzed Organic Carbon concentration (IMPROVE Protocol)	µg/m^3
OPTU	Pyrolyzed Organic Carbon concentration (IMPROVE Protocol) uncertainty	µg/m^3
OCTC	Organic Carbon concentration (IMPROVE Protocol)	µg/m^3
OCTU	Organic Carbon concentration (IMPROVE Protocol) uncertainty	µg/m^3
E1TC	Elemental Carbon Fraction 1 concentration (IMPROVE Protocol)	µg/m^3
E1TU	Elemental Carbon Fraction 1 concentration (IMPROVE Protocol) uncertainty	µg/m^3
E2TC	Elemental Carbon Fraction 2 concentration (IMPROVE Protocol)	µg/m^3
E2TU	Elemental Carbon Fraction 2 concentration (IMPROVE Protocol) uncertainty	µg/m^3
E3TC	Elemental Carbon Fraction 3 concentration (IMPROVE Protocol)	µg/m^3
E3TU	Elemental Carbon Fraction 3 concentration (IMPROVE Protocol) uncertainty	µg/m^3
ECTC	Elemental Carbon concentration (IMPROVE Protocol)	µg/m^3
ECTU	Elemental Carbon concentration (IMPROVE Protocol) uncertainty	µg/m^3
TCTC	Total Carbon concentration (IMPROVE Protocol)	µg/m^3
TCTU	Total Carbon concentration (IMPROVE Protocol) uncertainty	µg/m^3
STNOCTC	Organic Carbon concentration (STN-TOT Protocol)	µg/m^3
STNOCTU	Organic Carbon concentration (STN-TOT Protocol) uncertainty	µg/m^3
STNECTC	Elemental Carbon concentration (STN-TOT Protocol)	µg/m^3
STNECTU	Elemental Carbon concentration (STN-TOT Protocol) uncertainty	µg/m^3
STNTCTC	Total Carbon concentration (STN-TOT Protocol)	µg/m^3
STNTCTU	Total Carbon concentration (STN-TOT Protocol) uncertainty	µg/m^3
NAXC	Sodium concentration	µg/m^3
NAXU	Sodium concentration uncertainty	µg/m^3
MGXC	Magnesium concentration	µg/m^3
MGXU	Magnesium concentration uncertainty	µg/m^3
ALXC	Aluminum concentration	µg/m^3
ALXU	Aluminum concentration uncertainty	µg/m^3
SIXC	Silicon concentration	µg/m^3
SIXU	Silicon concentration uncertainty	µg/m^3
PHXC	Phosphorous concentration	µg/m^3
PHXU	Phosphorous concentration uncertainty	µg/m^3
SUXC	Sulfur concentration	µg/m^3
SUXU	Sulfur concentration uncertainty	µg/m^3
CLXC	Chlorine concentration	µg/m^3
CLXU	Chlorine concentration uncertainty	µg/m^3
KPXC	Potassium concentration	µg/m^3
KPXU	Potassium concentration uncertainty	µg/m^3
CAXC	Calcium concentration	µg/m^3
CAXU	Calcium concentration uncertainty	µg/m^3
TIXC	Titanium concentration	µg/m^3
TIXU	Titanium concentration uncertainty	µg/m^3
VAXC	Vanadium concentration	µg/m^3
VAXU	Vanadium concentration uncertainty	µg/m^3
CRXC	Chromium concentration	µg/m^3
CRXU	Chromium concentration uncertainty	µg/m^3
MNXC	Manganese concentration	µg/m^3
MNXU	Manganese concentration uncertainty	µg/m^3
FEXC	Iron concentration	µg/m^3
FEXU	Iron concentration uncertainty	µg/m^3

Table 3-1. (continued)

Field Code	Description	Measurement Unit
COXC	Cobalt concentration	µg/m^3
COXU	Cobalt concentration uncertainty	µg/m^3
NIXC	Nickel concentration	µg/m^3
NIXU	Nickel concentration uncertainty	µg/m^3
CUXC	Copper concentration	µg/m^3
CUXU	Copper concentration uncertainty	µg/m^3
ZNXC	Zinc concentration	µg/m^3
ZNXU	Zinc concentration uncertainty	µg/m^3
GAXC	Gallium concentration	µg/m^3
GAXU	Gallium concentration uncertainty	µg/m^3
ASXC	Arsenic concentration	µg/m^3
ASXU	Arsenic concentration uncertainty	µg/m^3
SEXC	Selenium concentration	µg/m^3
SEXU	Selenium concentration uncertainty	µg/m^3
BRXC	Bromine concentration	µg/m^3
BRXU	Bromine concentration uncertainty	µg/m^3
RBXC	Rubidium concentration	µg/m^3
RBXU	Rubidium concentration uncertainty	µg/m^3
SRXC	Strontium concentration	µg/m^3
SRXU	Strontium concentration uncertainty	µg/m^3
YTXC	Yttrium concentration	µg/m^3
YTXU	Yttrium concentration uncertainty	µg/m^3
ZRXC	Zirconium concentration	µg/m^3
ZRXU	Zirconium concentration uncertainty	µg/m^3
MOXC	Molybdenum concentration	µg/m^3
MOXU	Molybdenum concentration uncertainty	µg/m^3
PDXC	Palladium concentration	µg/m^3
PDXU	Palladium concentration uncertainty	µg/m^3
AGXC	Silver concentration	µg/m^3
AGXU	Silver concentration uncertainty	µg/m^3
CDXC	Cadmium concentration	µg/m^3
CDXU	Cadmium concentration uncertainty	µg/m^3
INXC	Indium concentration	µg/m^3
INXU	Indium concentration uncertainty	µg/m^3
SNXC	Tin concentration	µg/m^3
SNXU	Tin concentration uncertainty	µg/m^3
SBXC	Antimony concentration	µg/m^3
SBXU	Antimony concentration uncertainty	µg/m^3
BAXC	Barium concentration	µg/m^3
BAXU	Barium concentration uncertainty	µg/m^3
LAXC	Lanthanum concentration	µg/m^3
LAXU	Lanthanum concentration uncertainty	µg/m^3
AUXC	Gold concentration	µg/m^3
AUXU	Gold concentration uncertainty	µg/m^3
HGXC	Mercury concentration	µg/m^3
HGXU	Mercury concentration uncertainty	µg/m^3
TLXC	Thallium concentration	µg/m^3
TLXU	Thallium concentration uncertainty	µg/m^3

Table 3-1. (continued)

Field Code	Description	Measurement Unit
PBXC	Lead concentration	$\mu g/m^3$
PBXU	Lead concentration uncertainty	$\mu g/m^3$
URXC	Uranium concentration	$\mu g/m^3$
URXU	Uranium concentration uncertainty	$\mu g/m^3$

Table 3-2 lists the contents of the final data file. Each observable is identified by a field name which follows a pattern for that type of observable. For example, in the filter-based aerosol concentration file, the first two characters represent the measured species (e.g., AL for aluminum, SI for silicon, CA for calcium), the third character designates the analysis method (i.e., "G" for gravimetric weighing, "X" for x-ray fluorescence analysis, "I" for ion chromatography, "A" for atomic absorption spectrophotometry, "C" for automated colorimetry, "T" for thermal/optical carbon analysis), and the last character uses a "C" to identify a species concentration or a "U" to identify the uncertainty (i.e., precision) of the

Table 3-2. Summary of $PM_{2.5}$ data files for the Twelve Month Particulate Matter Study in Hong Kong.

Category	Database File	Database Description
I. DATABASE DOCUMENTATION		
	HKEPDFLDNAME.XLS	Defines the field names, measurement units, and formats used in the ambient database
II. MASS AND CHEMICAL DATA		
	HKEPD- PM25.XLS	Contains 24-hour $PM_{2.5}$ mass and chemical data[a,b] collected with partisol filter samplers at three sites on every sixth day between 11/06/00 and 10/26/01.
III. DATABASE VALIDATION		
	FLDFLAGS.DOC	Contains the field sampling data validation flags
	CHEMFLAG.DOC	Contains the chemical analysis data validation flags

[a] Includes 40 elements (Na, Mg, Al, Si, P, S, Cl, K, Ca, Ti, V, Cr, Mn, Fe, Co, Ni, Cu, Zn, Ga, As, Se, Br, Rb, Sr, Y, Zr, Mo, Pd, Ag, Cd, In, Sn, Sb, Ba, La, Au, Hg, Tl, Pb, and U) by x-ray fluorescence.

[b] Includes chloride, nitrate, and sulfate by ion chromatography; ammonium by automated colorimetry; water-soluble sodium and potassium by atomic absorption spectrophotometry; and organic carbon, elemental carbon, eight carbon fractions (OC1, OC2, OC3, OC4, OP, EC1, EC2, and EC3) by thermal/optical reflectance following the IMPROVE protocol, and OC and EC by thermal/optical transmittance following the USEPA STN (Speciation Trends Network) protocol.

corresponding measurement. Each measurement method is associated with a separate validation field to document the sample validity for that method. Missing or invalidated measurements have been removed and replaced with –99. All times show the start and end of the sampling period.

3.2 Measurement and Analytical Specifications

Every measurement consists of: 1) a value; 2) a precision; 3) an accuracy; and 4) a validity (Hidy, 1985; Watson et al., 1989, 2001). The measurement methods described in Section 2 are used to obtain the value. Performance testing via regular submission of standards, blank analysis, and replicate analysis are used to estimate precision. These precisions are reported in the data files described in Section 3.1 so that they can be propagated through air quality models and used to evaluate how well different values compare with one another. The submission and evaluation of independent standards through quality audits are used to estimate accuracy. Validity applies both to the measurement method and to each measurement taken with that method. The validity of each measurement is indicated by appropriate flagging within the data base, while the validity of the methods has been evaluated in this study by tests described in Section 3.4.

3.2.1 Definitions of Measurement Attributes

The precision, accuracy, and validity of the Twelve Month Particulate Matter Study in Hong Kong aerosol measurements are defined as follows (Chow et al., 1993a):

- A **measurement** is an observation at a specific time and place which possesses: 1) value – the center of the measurement interval; 2) precision – the width of the measurement interval; 3) accuracy – the difference between measured and reference values; and 4) validity – the compliance with assumptions made in the measurement method.

  A **measurement method** is the combination of equipment, reagents, and procedures, which provide the value of a measurement. The full description of the measurement method requires substantial documentation. For example, two methods may use the same sampling systems and the same analysis systems. These are not identical methods, however, if one performs acceptance testing on filter media and the other does not. Seemingly minor differences between methods can result in major differences between measurement values.

- **Measurement method validity** is the identification of measurement method assumptions, the quantification of effects of deviations from those assumptions, the evaluation that deviations are within reasonable tolerances for the specific application, and the creation of procedures to quantify and minimize those deviations during a specific application.

- **Sample validation** is accomplished by procedures that identify deviations from measurement assumptions and the assignment of flags to individual measurements for potential deviations from assumptions.

- The **comparability and equivalence of sampling and analysis methods** are established by the comparison of values and precisions for the same measurement obtained by different measurement methods. Interlaboratory and intralaboratory comparisons are usually made to establish this comparability. Simultaneous measurements of the same observable are considered equivalent when more than 90% of the values differ by no more than the sum of two one-sigma precision intervals for each measurement.

- **Completeness** measures how many environmental measurements with specified values, precisions, accuracies, and validities were obtained out of the total number attainable. It measures the practicability of applying the selected measurement processes throughout the measurement period. Databases which have excellent precision, accuracy, and validity may be of little use if they contain so many missing values that data interpretation is impossible.

A total of 180 filter samples were acquired during this study, and 176 samples were submitted for comprehensive chemical analyses. This resulted in about 10,000 data points, as documented in Section 3.1. All of the 176 ambient aerosol samples acquired during the study were considered valid after data validation and final review.

A database with numerous data points, such as the one generated from this study, requires detailed documentation of precision, accuracy, and validity of the measurements. The next section addresses the procedures followed to define these quantities and presents the results of the procedures.

3.2.2 Definitions of Measurement Precision

Measurement precisions were propagated from precisions of the volumetric measurements, the chemical composition measurements, and the field blank variability using the methods of Bevington (1969) and Watson et al. (2001). The following equations calculated the precision associated with filter-based measurements:

$$C_i = (M_i - B_i)/V \quad (3\text{-}1)$$

$$V = F \times t \quad (3\text{-}2)$$

$$B_i = \frac{1}{n}\sum_{j=1}^{n} B_{ij} \quad \text{for } B_i > \sigma_{Bi} \quad (3\text{-}3)$$

$$B_i = 0 \quad \text{for } B_i \le \sigma_{Bi} \quad (3\text{-}4)$$

$$\sigma_{Bi} = STD_{Bi} = \left[\frac{1}{n-1}\sum_{j=1}^{n}(B_{ij} - B_i)^2\right]^{1/2} \quad \text{for } STD_{Bi} > SIG_{Bi} \quad (3\text{-}5)$$

$$\sigma_{Bi} = SIG_{Bi} = \left[\frac{1}{n}\sum_{j=1}^{n}(s_{Bij})^2\right]^{1/2} \quad \text{for } STD_{Bi} \le SIG_{4Bi} \quad (3\text{-}6)$$

$$\sigma_{Ci} = \left[\frac{s_{Mi}^2 + s_{Bi}^2}{V^2} + \frac{s_V^2 (M_i - B_i)^2}{V^4}\right]^{1/2} \quad (3\text{-}7)$$

$$\sigma_{RMS_i} = \left(\frac{1}{n}\sum_{j=1}^{n} s_{Ci}^2\right)^{1/2} \quad (3\text{-}8)$$

$$\sigma_V/V = 0.05 \quad (3\text{-}9)$$

where:

B_i = average amount of species i on field blanks

B_{ij} = the amount of species i found on field blank j

C_i = the ambient concentration of species i

F = flow rate throughout sampling period

M_i = amount of species i on the substrate

M_{ijf} = amount of species i on sample j from original analysis

M_{ijr} = amount of species i on sample j from replicate analysis

n = total number of samples in the sum

SIG_{Bi} = the root mean square error (RMSE), the square root of the averaged sum of the squared of σ_{Bij}.

STD_{Bi} = standard deviation of the blank

σ_{Bi} = blank precision for species i

σ_{Bij} = precision of the species i found on field blank j

σ_{Ci} = propagated precision for the concentration of species i

σ_{Mi} = precision of amount of species i on the substrate

σ_{RMS_i} = root mean square precision for species i

σ_V = precision of sample volume

t = sample duration

V = volume of air sampled

Dynamic field blanks were periodically placed in each sampling system without air being drawn through them to estimate the magnitude of passive deposition for the period of time which filter packs remained in a sampler (typically 24 hours). No statistically significant inter-site differences in field blank concentrations were found for any species after removal of outliers (i.e., concentration exceeding three times the standard deviations of the field blanks). The average field blank concentrations (with outliers removed) were calculated for each species on each substrate (e.g., Teflon-membrane, quartz-fiber), irrespective of the sites.

3.2.3 Analytical Specifications

Blank precisions (σ_{Bi}) are defined as the higher value of the standard deviation of the blank measurements, STD_{Bi}, or the square root of the averaged squared uncertainties of the blank concentrations, SIG_{Bi}. If the average blank for a species was less than its precision, the blank was set to zero (as shown in Equation 3-4). Dynamic field blank concentrations in µg/filter are given in Table 3-3 for $PM_{2.5}$ samples collected during the study.

The precisions (σ_{Mi}) for x-ray fluorescence analysis were determined from counting statistics unique to each sample. Hence, the σ_{Mi} is a function of the energy-specific peak area, the background, and the area under the baseline.

As shown in Table 3-3, the standard deviation of the field blank is more than twice its corresponding root mean square error (RMSE) for soluble sodium (Na^+) and soluble potassium (K^+). Some of these field blanks may have been contaminated during the passive deposition period and during sample changing while exposed to ambient conditions. By examining the individual field blank values, it is shown that these values are well within the range of the standard deviation of the average blank concentrations and therefore are assumed valid and representative.

$PM_{2.5}$ Teflon mass blank values averaged 0.77±2.9 µg/47-mm filter. The quartz mass blank values averaged 29.8±35.0 µg/47-mm filter. Filter mass and blank mass analysis was performed by the HKEPD. Blank subtractions and calculated uncertainties were not examined by DRI and were thus not included in Table 3-3 and 3-4. The largest variation was found for soluble sodium, with an average of 23.2±6.3 µg/47-mm filter. This large standard deviation in blank samples was mainly due to the adsorption of sodium chloride during the passive sampling period when filters were left in the sampler prior to and after sampling. The proximity of the sampling sites to the ocean (<1 km) supports this assumption. These deviations were equivalent for both field and laboratory filter blanks. However, only about 10% of the sodium contamination (deviation) is explained by the chloride deviation.

Table 3-4 summarizes the analytical specifications for the 24-hour $PM_{2.5}$ measurements obtained during the study. Minimum detectable limits (MDL), root mean squared (RMS) precisions, and lower quantifiable limits (LQL) are given. The MDL is defined as the concentration at which the instrument response equals three times the standard deviation of the response to a known concentration of zero. RMS precision is the square root

Table 3-3. $PM_{2.5}$ Partisol dynamic field blank concentrations at the MK, TW and HT sites during the Twelve Month Particulate Matter Study in Hong Kong.

	Concentrations in µg/47-mm filter					
Species	Blank Subtracted[a] (B_i)	Blank Subtracted Precision[b] (s_{Bi})	Average Field Blank	Field Blank Std. Dev. (STD_{Bi})	Root Mean Squared Blank Precision[c] (s_{RMS})	Total No. of Blanks in Average
Teflon Mass	0.0000	2.8832**	0.7733	2.8832**	5.500**	75
Quartz Mass	0.0000	34.9969**	29.8169	34.9969**	5.500**	71
Chloride (Cl^-)	1.0827	0.6821	1.0827	0.6161	0.6821	71
Nonvolatilized Nitrate (NO_3^-)	0.0000	0.6600	0.1012	0.3009	0.6600	71
Sulfate ($SO_4^=$)	2.6601	1.2151	2.6601	1.2151	0.6701	70
Ammonium (NH_4^+)	0.8708	0.6608	0.8708	0.2665	0.6608	71
Soluble Sodium (Na^+)	23.2037	6.2905	23.2037	6.2905	0.2702	71
Soluble Potassium (K^+)	0.3859	0.1884	0.3859	0.1884	0.0680	71
IMPROVE PROTOCOL						
O1TC	1.7699	1.3529	1.7699	1.3529	0.5894	70
O2TC	3.8513	1.4509	3.8513	1.4509	0.8606	70
O3TC	6.3430	2.3703	6.3430	1.5513	2.3703	70
O4TC	0.0000	1.0259	0.9879	1.0259	0.8835	70
OPTC	0.0000	0.6400	0.0027	0.0177	0.6400	70
OCTC	12.9600	3.3319	12.9600	3.3286	3.3319	70
E1TC	0.0000	0.5240	0.1391	0.5240	0.4819	70
E2TC	0.0000	1.0393	0.4190	1.0393	0.6511	70
E3TC	0.0000	0.2008	0.0187	0.1365	0.2008	70
ECTC	0.0000	1.2688	0.5743	1.2688	0.8000	70
TCTC	13.5329	4.0608	13.5329	4.0608	3.7332	70
STN PROTOCOL						
OCTC	25.6600	4.9388	25.6600	4.9388	3.4675	60
ECTC	2.1317	1.3783	2.1317	1.3783	0.7670	60
TCTC	27.7800	5.6266	27.7800	5.6266	3.8674	60
Sodium (Na)	0.2942	0.3422	0.2942	0.2871	0.3422	75
Magnesium (Mg)	0.0000	0.1955	0.1426	0.1428	0.1955	75
Aluminum (Al)	0.0000	0.1140	0.0877	0.0868	0.1140	75
Silicon (Si)	0.0000	0.1138	0.0996	0.1138	0.0687	75
Phosphorus (P)	0.0462	0.0567	0.0462	0.0341	0.0567	75
Sulfur (S)	0.0481	0.0602	0.0481	0.0443	0.0602	75
Chlorine (Cl)	0.0000	0.1188	–0.0035	0.0617	0.1188	75
Potassium (K)	0.0000	0.1115	–0.0293	0.0649	0.1115	75
Calcium (Ca)	0.0000	0.1269	–0.0194	0.0536	0.1269	75
Titanium (Ti)	0.0000	0.5158	–0.0786	0.1305	0.5158	75

Table 3-3. (continued)

Species	Concentrations in µg/47-mm filter: Blank Subtracted[a] (B_j)	Blank Subtracted Precision[b] (s_{Bi})	Average Field Blank	Field Blank Std. Dev. (STD_{Bi})	Root Mean Squared Blank Precision[c] (s_{RMS})	Total No. of Blanks in Average
Vanadium (V)	0.0000	0.2349	–0.0465	0.0814	0.2349	75
Chromium (Cr)	0.0000	0.0605	–0.0067	0.0245	0.0605	75
Manganese (Mn)	0.0000	0.0361	–0.0026	0.0129	0.0361	75
Iron (Fe)	0.0000	0.0271	0.0063	0.0197	0.0271	75
Cobalt (Co)	0.0000	0.0204	0.0007	0.0053	0.0204	75
Nickel (Ni)	0.0000	0.0197	0.0011	0.0062	0.0197	75
Copper (Cu)	0.0000	0.0228	0.0030	0.0129	0.0228	75
Zinc (Zn)	0.0000	0.0232	0.0080	0.0165	0.0232	75
Gallium (Ga)	0.0000	0.0372	–0.0013	0.0130	0.0372	75
Arsenic (As)	0.0000	0.0426	–0.0039	0.0085	0.0426	75
Selenium (Se)	0.0000	0.0237	–0.0020	0.0056	0.0237	75
Bromine (Br)	0.0000	0.0213	0.0008	0.0065	0.0213	75
Rubidium (Rb)	0.0000	0.0196	–0.0008	0.0047	0.0196	75
Strontium (Sr)	0.0000	0.0219	–0.0012	0.0049	0.0219	75
Yttrium (Y)	0.0000	0.0268	–0.0002	0.0068	0.0268	75
Zerconium (Zr)	0.0000	0.0315	–0.0015	0.0083	0.0315	75
Molybdenum (Mo)	0.0000	0.0566	0.0029	0.0148	0.0566	75
Palladium (Pd)	0.0000	0.1649	0.0164	0.0527	0.1649	75
Silver (Ag)	0.0000	0.1977	–0.0064	0.0775	0.1977	75
Cadmium (Cd)	0.0000	0.2093	–0.0082	0.0732	0.2093	75
Indium (In)	0.0000	0.2363	0.0254	0.0683	0.2363	75
Tin (Sn)	0.0000	0.2958	0.0070	0.1065	0.2958	75
Antimony (Sb)	0.0000	0.3553	0.0007	0.1382	0.3553	75
Barium (Ba)	0.0000	1.3002	0.0301	0.4695	1.3002	75
Lanthanum (La)	0.0000	1.7694	0.1010	0.6155	1.7694	75
Gold (Au)	0.0000	0.0600	–0.0018	0.0237	0.0600	75
Mercury (Hg)	0.0000	0.0509	–0.0034	0.0129	0.0509	75
Thallium (Tl)	0.0000	0.0503	–0.0029	0.0129	0.0503	75
Lead (Pb)	0.0000	0.0663	–0.0019	0.0247	0.0663	75
Uranium (U)	0.0000	0.0480	–0.0038	0.0130	0.0480	75

** DRI did not conduct filter mass analysis. Estimated mass precision is given.

[a] Values used in data processing. Non-zero average blank concentrations are subtracted when the average blank exceeds its standard deviation.

[b] Larger of either the analytical precision or standard deviation from the field.

[c] RMS precision is the square root of the sum of the squared uncertainties of the observations divided by the number of observations.

Table 3-4. Analytical specifications for 24-hour $PM_{2.5}$ measurements at the MK, TW, and HT sites during the Twelve Month Particulate Matter Study in Hong Kong.

Species	Analysis Method[a]	MDL[b] (µg/m^3)	RMS[c] (µg/m^3)	LQL[d] (µg/m^3)	No. of Values[e]	No. > MDL	% > MDL	No. > LQL	% > LQL
Teflon Mass	Gravimetry	N/A	4.6896	N/A	176	N/A	N/A	N/A	N/A
Quartz Mass	Gravimetry	N/A	4.7592	N/A	176	N/A	N/A	N/A	N/A
Chloride (Cl^-)	IC	0.0521	0.0573	0.1559	176	112	64%	65	37%
Nonvolatilized Nitrate (NO_3^-)	IC	0.0521	0.1226	0.0347	176	174	99%	175	99%
Sulfate ($SO_4^=$)	IC	0.0521	1.0807	0.0347	176	176	100%	176	100%
Ammonium (NH_4^+)	AC	0.0521	0.2080	0.0348	176	174	99%	175	99%
Soluble Sodium (Na^+)	AAS	0.0104	0.2637	0.0192	176	164	93%	162	92%
Soluble Potassium (K^+)	AAS	0.0104	0.0370	0.0090	176	176	100%	176	100%
IMPROVE TOR PROTOCOL									
O1TC	TOR	0.0958	0.5894	0.1123	129	104	81%	102	79%
O2TC	TOR	0.0958	0.8606	0.1204	129	129	100%	129	100%
O3TC	TOR	0.0958	2.3703	0.1967	129	129	100%	127	98%
O4TC	TOR	0.0958	0.8835	0.0851	129	129	100%	129	100%
OPTC	TOR	0.0958	0.6400	0.0531	129	17	13%	22	17%
OCTC	TOR	0.0958	3.3319	0.2765	129	129	100%	129	100%
E1TC	TOR	0.0958	0.4819	0.0435	129	129	100%	129	100%
E2TC	TOR	0.0958	0.6511	0.0862	129	122	95%	125	97%
E3TC	TOR	0.0958	0.2008	0.0167	129	1	1%	3	2%
ECTC	TOR	0.0958	0.8000	0.1053	129	129	100%	129	100%
TCTC	TOR	0.0958	3.7332	0.3370	129	129	100%	129	100%
STN TOT PROTOCOL									
OCTC	TOT	0.0958	3.4675	0.4099	129	128	99%	128	99%
ECTC	TOT	0.0958	0.7670	0.1144	129	128	99%	128	99%
TCTC	TOT	0.0958	3.8674	0.4669	129	128	99%	128	99%
Sodium (Na)	XRF	0.0331	0.0423	0.2031	176	162	92%	86	49%
Magnesium (Mg)	XRF	0.012	0.0211	0.0302	176	155	88%	116	66%
Aluminum (Al)	XRF	0.0048	0.0122	0.0156	176	174	99%	163	93%
Silicon (Si)	XRF	0.003	0.0284	0.0374	176	176	100%	172	98%
Phosphorus (P)	XRF	0.0027	0.0148	0.0047	176	96	55%	81	46%
Sulfur (S)	XRF	0.0024	0.1883	0.0041	176	176	100%	176	100%
Chlorine (Cl)	XRF	0.0048	0.0655	0.0099	176	90	51%	82	47%
Potassium (K)	XRF	0.0029	0.0368	0.0083	176	176	100%	176	100%
Calcium (Ca)	XRF	0.0022	0.0114	0.0201	176	176	100%	172	98%
Titanium (Ti)	XRF	0.0014	0.0317	0.0363	176	123	70%	6	3%
Vanadium (V)	XRF	0.0012	0.0133	0.0166	176	155	88%	46	26%
Chromium (Cr)	XRF	0.0009	0.0038	0.0042	176	66	38%	3	2%
Manganese (Mn)	XRF	0.0008	0.0019	0.0024	176	169	96%	156	89%
Iron (Fe)	XRF	0.0007	0.0123	0.0068	176	176	100%	174	99%
Cobalt (Co)	XRF	0.0004	0.0040	0.0014	176	23	13%	2	1%
Nickel (Ni)	XRF	0.0004	0.0010	0.0013	176	172	98%	158	90%
Copper (Cu)	XRF	0.0005	0.0013	0.0015	176	164	93%	156	89%
Zinc (Zn)	XRF	0.0005	0.0105	0.0016	176	175	99%	174	99%
Gallium (Ga)	XRF	0.0009	0.0026	0.0025	176	33	19%	4	2%
Arsenic (As)	XRF	0.0008	0.0152	0.0028	176	135	77%	96	55%
Selenium (Se)	XRF	0.0006	0.0013	0.0015	176	136	77%	94	53%

Table 3-4. (continued)

Species	Analysis Method[a]	MDL[b] (μg/m^3)	RMS[c] (μg/m^3)	LQL[d] (μg/m^3)	No. of Values[e]	No. > MDL	% > MDL	No. > LQL	% > LQL
Bromine (Br)	XRF	0.0005	0.0015	0.0014	176	176	100%	174	99%
Rubidium (Rb)	XRF	0.0005	0.0011	0.0013	176	135	77%	120	68%
Strontium (Sr)	XRF	0.0005	0.0013	0.0015	176	120	68%	53	30%
Yttrium (Y)	XRF	0.0006	0.0019	0.0018	176	3	2%	0	0%
Zerconium (Zr)	XRF	0.0008	0.0020	0.0021	176	43	24%	4	2%
Molybdenum (Mo)	XRF	0.0013	0.0036	0.0039	176	21	12%	0	0%
Palladium (Pd)	XRF	0.0053	0.0104	0.0107	176	6	3%	0	0%
Silver (Ag)	XRF	0.0058	0.0124	0.0127	176	8	5%	0	0%
Cadmium (Cd)	XRF	0.0058	0.0131	0.0133	176	22	13%	0	0%
Indium (In)	XRF	0.0062	0.0147	0.0147	176	12	7%	0	0%
Tin (Sn)	XRF	0.0081	0.0159	0.0193	176	127	72%	61	35%
Antimony (Sb)	XRF	0.0086	0.0220	0.0227	176	27	15%	2	1%
Barium (Ba)	XRF	0.0249	0.0805	0.0867	176	57	32%	0	0%
Lanthanum (La)	XRF	0.0297	0.1101	0.1182	176	27	15%	0	0%
Gold (Au)	XRF	0.0015	0.0080	0.0039	176	18	10%	2	1%
Mercury (Hg)	XRF	0.0012	0.0033	0.0032	176	3	2%	0	0%
Thallium (Tl)	XRF	0.0012	0.0043	0.0031	176	1	1%	0	0%
Lead (Pb)	XRF	0.0014	0.0060	0.0044	176	171	97%	162	92%
Uranium (U)	XRF	0.0011	0.0032	0.0032	176	3	2%	0	0%

[a] IC=ion chromatography. AC=automated colorimetry. AAS=atomic absorption spectrophotometry. TOR= thermal/optical reflectance. XRF=x-ray fluorescence.

[b] Minimum detectable limit (MDL) is the concentration at which instrument response equals three times the standard deviation of the response to a known concentration of zero. Typical sample volumes are 24.1 m^3.

[c] Root mean squared precision (RMS) is the square root of the sum of the squared uncertainties of the observations divided by the number of observations.

[d] Lower quantifiable limit (LQL) is two times the uncertainty of the field blank. LQL is expressed here in terms of mass per cubic meter after dividing by 24.1 m^3 for Partisol samplers.

[e] Number of non-void values (with -99) reported.

of the averaged squared uncertainties. The LQL is defined as a concentration corresponding to two times the precision of the dynamic field blank. The LQLs in Table 3-4 were divided by 24.1 m^3, nominal 24-hour volume, for the Partisol samplers. Actual volumes varied from sample to sample, but were typically within ±5% of the pre-set volume. The LQLs should always be equal to or larger than the analytical MDLs because they include the standard deviation of the field blank and flow rate precision (Watson et al., 2001). This was the case for most of the chemical compounds noted in Table 3-4. This table also indicates that the RMS precisions were comparable in magnitude to the LQLs for most species.

The number of reported (nonvoid, nonmissing) concentrations for each species and the number of reported concentrations greater than the MDLs and LQLs are also summarized in Table 3-4. For the study samples, mass, ions (e.g., nonvolatilized nitrate, sulfate, ammonium, and soluble potassium), organic and elemental carbon, sulfur, and lead were

detected in almost all samples (greater than 95%). Chloride and soluble sodium were detected in 64% and 93% of the samples, respectively. Several transition metals (e.g., Co, Y, Mo, Pd, Ag, Cd, In, Sb, La, Au, Hg, Tl, and U) were not detected in most of the samples (less than 15%). This is typical for urban and non-urban sites in most regions. Other transition metals, such as titanium (Ti), chromium (Cr), copper (Cu), gallium (Ga), arsenic (As), selenium (Se), rubidium (Rb), zirconium (Zr), strontium (Sr), tin (Sn) and, barium (Ba), were detected in 70%, 38%, 93%, 19%, 77%, 77%, 77%, 24% 68%, 72%, and 32% of the analyzed samples. These metals were above the LQLs in 3%, 2%, 89%, 2%, 55%, 53%, 68%, 2%, 30%, 35%, and 0%, respectively. Residual-oil-related species, such as nickel (Ni) and vanadium (V), were detected in 98% and 88% of the samples, respectively. Industrial-source-related toxic species such as mercury (Hg) and cadmium (Cd) were only detected in 2% and 13% of the samples, respectively. Arsenic (As) and selenium (Se) were found above the MDLs in 77% of the samples. The maximum arsenic (As) concentration of 0.0496 $\mu g/m^3$ is a fairly high value, being over 20 times higher than the maximum concentration measured during the 2000-01 Southern Nevada Air Quality Study (SNAQS, Green et al., 2002) in the U.S. Crustal-related species such as aluminum (Al), silicon (Si), potassium (K), calcium (Ca), manganese (Mn), iron (Fe), and zinc (Zn) were found above the MDLs in over 96% of the samples and above the LQLs in more than 89% of the samples. Motor-vehicle-related species such as bromine (Br) and lead (Pb) were detected in 100% and 97% of the samples, respectively. Chlorine was detected in over half of the samples.

These analytical specifications imply that $PM_{2.5}$ samples acquired during the study possess adequate sample loading for chemical analysis of those species that are expected from sources in the region. In addition, the MDLs of the selected chemical analysis methods were sufficiently low to establish valid measurements with acceptable precisions.

3.3 Quality Assurance

Quality control (QC) and quality auditing establish the precision, accuracy, and validity of measured values. Quality assurance integrates quality control, quality auditing, measurement method validation, and sample validation into the measurement process. The results of quality assurance are data values with specified precisions, accuracies, and validities.

Quality control (QC) is intended to prevent, identify, correct, and define the consequences of difficulties that might affect the precision and accuracy, and or validity of the measurements. Quality auditing consisted of systems and performance audits. The system audit should include a review of the operational and QC procedures to assess whether they were adequate to assure valid data that met the specified levels of accuracy and precision. Quality auditing should also examine all phases of the measurement activity to determine that procedures were followed and that operators were properly trained. Performance audits should establish whether the predetermined specifications were achieved in practice. The performance audits should challenge the measurement/analysis systems with known transfer standards traceable to primary standards. Quality Control and Quality Auditing procedures were carried out by the HKEPD for the samplers and for filter mass analyses. Both system and performance audits were performed in DRI's Environmental

Analysis Facility on an annual basis to assure data quality. Auditors acquired and reviewed the standard operating procedures and examined all phases of measurement activities to assure that procedures were followed and that operators were properly trained.

Field blanks were acquired and replicate analyses was performed for ~15% of all ambient samples. As previously mentioned, quality assurance audits of sample flow rates were conducted by the HKEPD throughout the study period. The audit results are not included in this report but are available from the HKEPD. Data were submitted at two levels of data validation (Chow et al., 1994, Watson et al., 2001). Detailed data validation processes are documented in the following subsections.

3.4 Data Validation

Data acquired from the study was submitted to three data validation levels:

- Level 0 sample validation designates data as they come off the instrument. This process ascertains that the field or laboratory instrument is functioning properly.

- Level I sample validation: 1) flags samples when significant deviations from measurement assumptions have occurred, 2) verifies computer file entries against data sheets, 3) eliminates values for measurements that are known to be invalid because of instrument malfunctions, 4) replaces data from a backup data acquisition system in the event of failure of the primary system, and 5) adjusts values for quantifiable calibration or interference biases.

- Level II sample validation applies consistency tests to the assembled data based on known physical relationships between variables.

- Level III sample validation is part of the data interpretation process. The first assumption upon finding a measurement which is inconsistent with physical expectations, is that the unusual value is due to a measurement error. If, upon tracing the path of the measurement nothing unusual is found, the value can be assumed to be a valid result of an environmental cause. Unusual values are identified during the data interpretation process as: 1) extreme values, 2) values which would otherwise normally track the values of other variables in a time series, and 3) values for observables which would normally follow a qualitatively predictable spatial or temporal pattern.

Level I validation flags and comments are included with each data record in the data base as documented in Section 3.1. Level II validation tests and results are described in the following subsections. Level III data validation will not be completed until further data analysis is performed.

Level II tests evaluate the chemical data for internal consistency. In this study, Level II data validations were made for: 1) sum of chemical species versus $PM_{2.5}$ mass, 2) physical consistency, 3) anion and cation balance, and 4) reconstructed versus measured mass.

Correlations and linear regression statistics were computed and scatter plots prepared to examine the data.

3.4.1 Sum of Chemical Species versus Mass

The sum of the individual chemical concentrations for $PM_{2.5}$ should be less than or equal to the corresponding gravimetrically measured mass concentrations. This sum includes chemicals quantified on the Teflon-membrane and quartz-fiber filters. Total sulfur (S), soluble chloride (Cl^-), and soluble potassium (K^+) are excluded from the sum to avoid double counting since sulfate ($SO_4^=$), chlorine (Cl), and total potassium (K) are included in the sum. Elemental sodium (Na) and magnesium (Mg) have low atomic numbers and require detailed particle size distributions in order to completely correct for particle x-ray absorption effects, so these concentrations are also excluded from the calculation. Measured concentrations do not account for unmeasured metal oxides in crustal material, unmeasured cations, or hydrogen and oxygen associated with organic carbon.

Figure 3-2 shows scatter plots of the $PM_{2.5}$ sum of species versus mass on Teflon filters for all the sites combined and for each of the individual sites. Each plot contains a

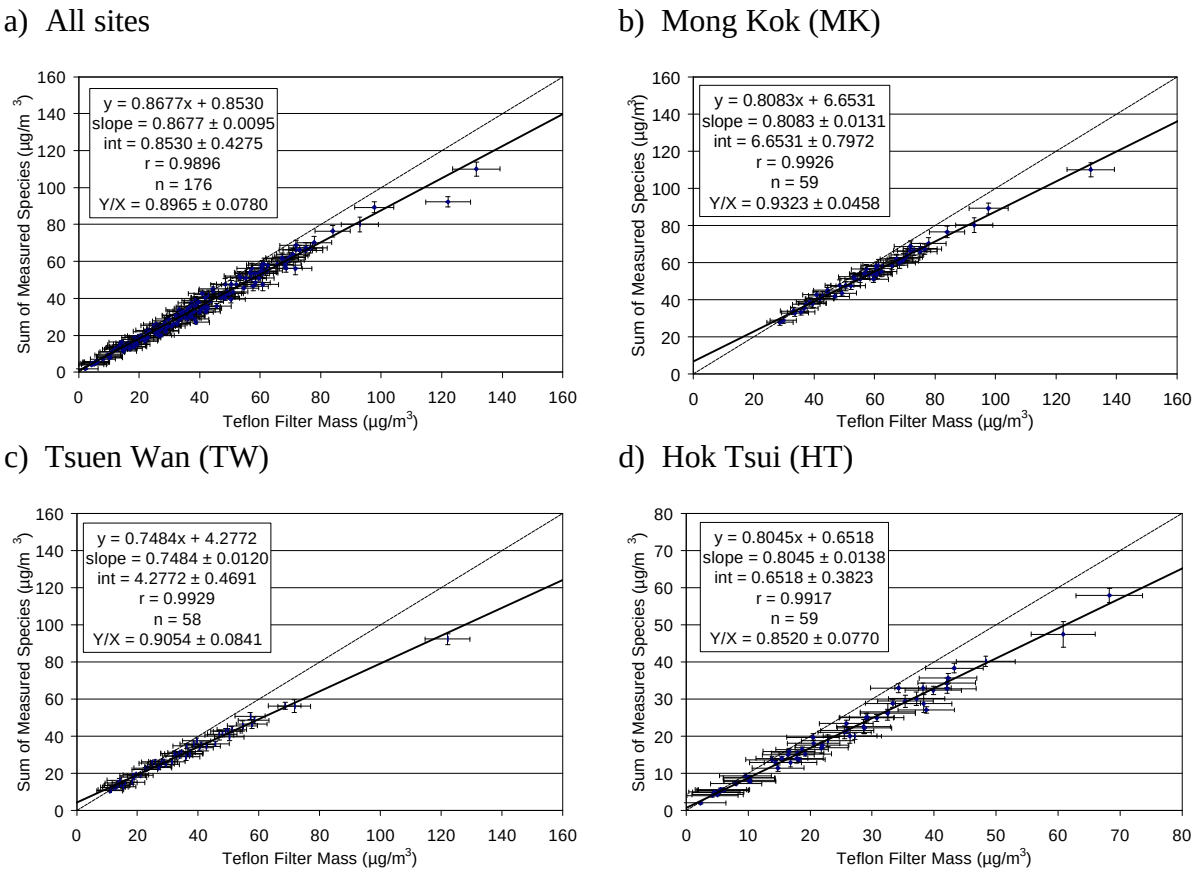

Figure 3-2. Scatter plots of sum of species versus mass measurements from $PM_{2.5}$ data acquired at: a) all three sites; b) the MK site; c) the TW site; and d), the HT site.

solid line indicating the slope with intercept and a dashed one-to-one line. Measurement uncertainties associated with the x- and y-axes are shown for comparison. Regression statistics with mass as the independent variable (X) and sum of species as the dependent variable (Y) are also calculated. The calculated correlation coefficient and number of data points is also shown for comparison, as is the average of the ratios of Y over X. As intercepts are low compared to the measured concentrations, the slope closely represents the ratio of Y over X. Any suspect data were examined, flagged, and removed if applicable from statistical analysis when sampling or analytical anomalies were identified.

As shown by Figure 3-2a, all of the sums are less than the corresponding $PM_{2.5}$ mass within the reported precisions. An excellent relationship was found between the sum of species and mass, with correlation coefficients exceeding 0.98 for the all measurements. Approximately 90% of the $PM_{2.5}$ mass was explained by the chemical species measured during the study.

Comparisons among the individual sites were similar. Figures 3-2b, c, and d show that all $PM_{2.5}$ measurements are below the one-to-one line within measurement uncertainties. High correlations ($r=>0.99$) are also seen for all of the sites. These comparisons are also very similar, with the exception of the HT background site which exhibited much lower mass concentrations. The intercept coefficient for the HT background site is much closer to zero than the intercept for the other two sites. Since organic carbon is often a large portion of $PM_{2.5}$ mass, the elevated sum of species was affected by high carbon mass at the MK and TW sites.

3.4.2 Physical Consistency

The composition of chemical species concentrations measured by different chemical analysis methods was examined. Physical consistency was tested for: 1) sulfate versus total sulfur, 2) chloride versus chlorine, and 3) soluble potassium versus total potassium.

3.4.2.1 Sulfate versus Total Sulfur

Water-soluble sulfate ($SO_4^{=}$) was measured by ion chromatography (IC) analysis on quartz-fiber filters, and total sulfur (S) was measured by x-ray fluorescence (XRF) analysis on Teflon-membrane filters. The ratio of sulfate to total sulfur should equal "3" if all of the sulfur were present as soluble sulfate. Figure 3-3a shows scatter plots of sulfate versus sulfur concentrations for all three sites. A good correlation ($r>0.98$) was found among $PM_{2.5}$ sulfur/sulfate measurements with an average ratio of 2.74±0.24.

High correlations ($r>0.98$) were found for $PM_{2.5}$ sulfate/sulfur comparisons among the individual sites. Figures 3-3b, c, and d show that all but a few of the data pairs fell beyond the three-to-one line. The regression statistics give a slope ranging from 2.79±0.07 to 2.85±0.07 with negligible intercepts (maximum of –0.44±0.27 $\mu g/m^3$). Overall, the sulfate and total sulfur comparisons in this study support the contentions that more than 90% of sulfur was present as soluble sulfate in the atmosphere and that both XRF and IC measurements are valid.

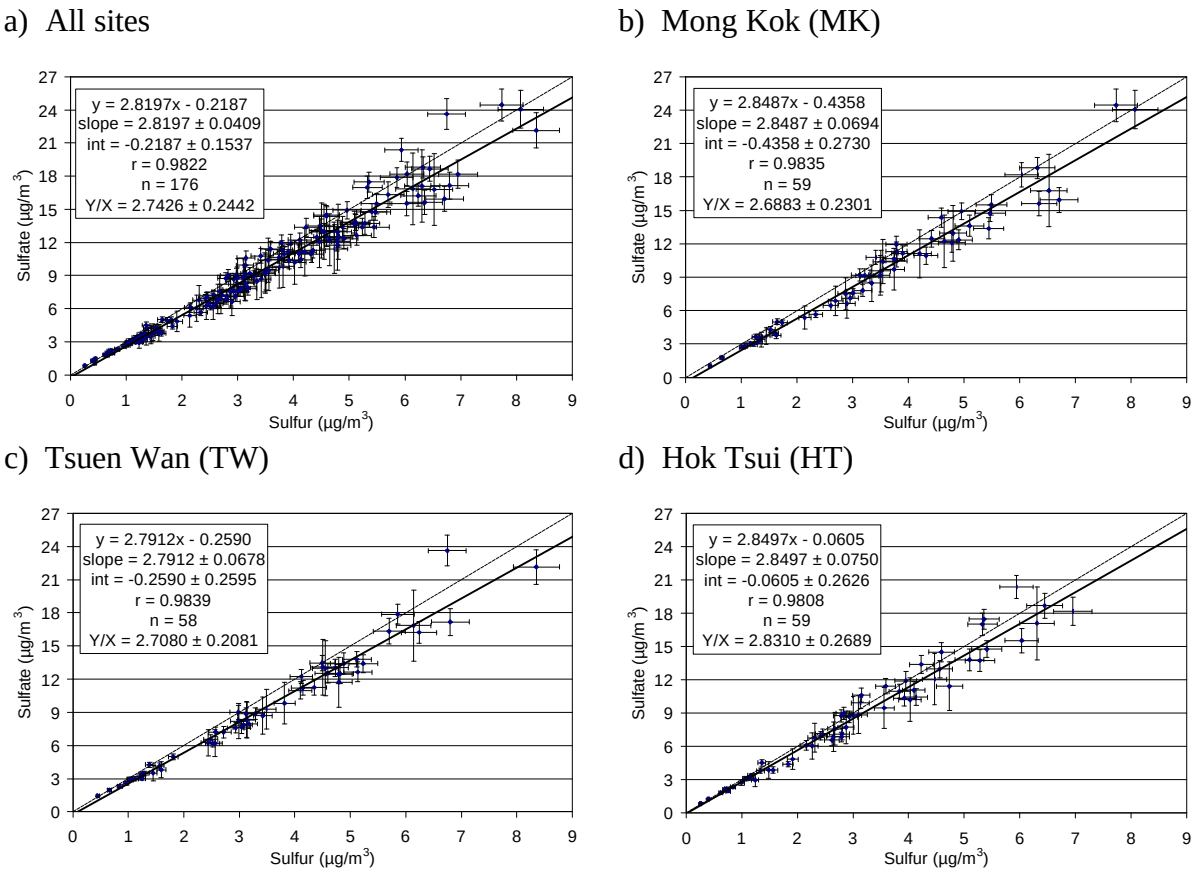

Figure 3-3. Scatter plots of sulfate versus sulfur measurements from $PM_{2.5}$ data acquired at: a) all three sites; b) the MK site; c) the TW site; and d) the HT site.

3.4.2.2 Chloride versus Chlorine

Chloride (Cl^-) was measured by IC on quartz-fiber filters, and chlorine (Cl) was measured by XRF on Teflon-membrane filters. Because chloride is the water-soluble portion of chlorine, the chloride-to-chlorine ratio is expected to be less than unity. Figure 3-4a shows that moderate correlations (r=0.90) were found between $PM_{2.5}$ chloride and chlorine measurements, with a slope close to unity and low intercepts for all of the sites. The uncertainties of chloride measurements were higher at low concentrations because chloride's elution peak in ion chromatographic analysis is close to the distilled water dip which, in turn, shifts the baseline of the chromatogram (Chow and Watson, 1999). In addition, chlorine collected on the Teflon filter may be lost through volatilization because XRF analysis is conducted in a vacuum chamber. Such losses are especially apparent when chlorine concentrations are low.

a) All sites

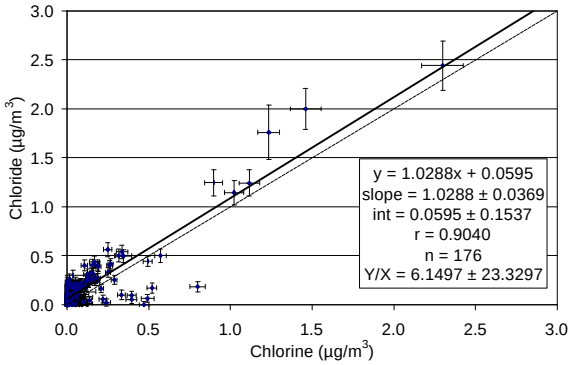

b) Mong Kok (MK)

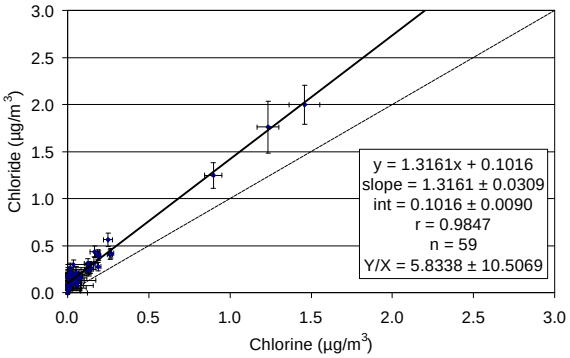

c) Tsuen Wan (TW)

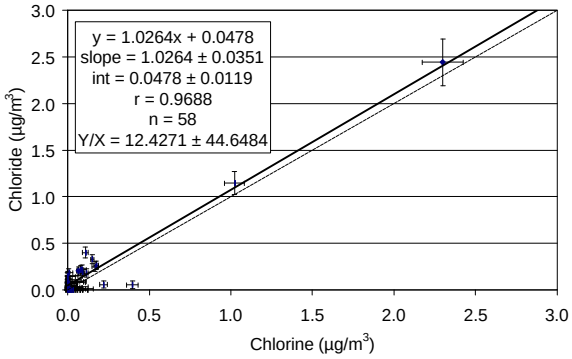

d) Hok Tsui (HT)

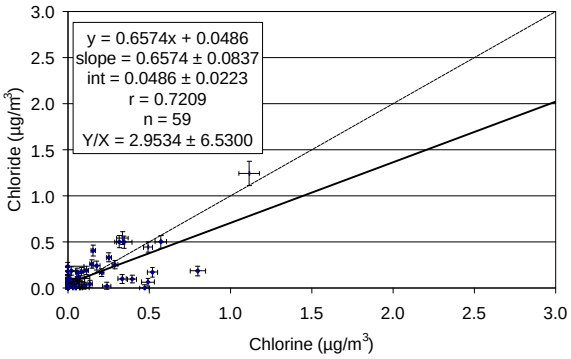

Figure 3-4. Scatter plots of chloride versus chlorine measurements from $PM_{2.5}$ data acquired at: a) all three sites; b) the MK site; c) the TW site; and d), the HT site.

3.4.2.3 Soluble Potassium versus Total Potassium

Soluble potassium (K^+) was acquired by atomic absorption spectrophotometry (AAS) analysis on quartz-fiber filters, and total potassium (K) was acquired by XRF analysis on Teflon-membrane filters. Since potassium concentrations are often used as an indicator of vegetative burning, it is important to assure the validity of the K^+ measurement.

Figure 3-5 displays the scatter plots of soluble potassium versus total potassium concentrations. Large uncertainty intervals associated with total potassium measurements reflected the uncertainty of light element particle corrections in x-ray fluorescence analysis. This analysis shows that K^+ concentrations are low to moderate throughout the study area, even though an average of 90% of the total potassium is in its soluble state. The average y/x ratio of K^+/K was 0.80±0.10. The higher K^+/K ratios imply that vegetative burning or long-range transport of wildfire emissions are prominent in the study area.

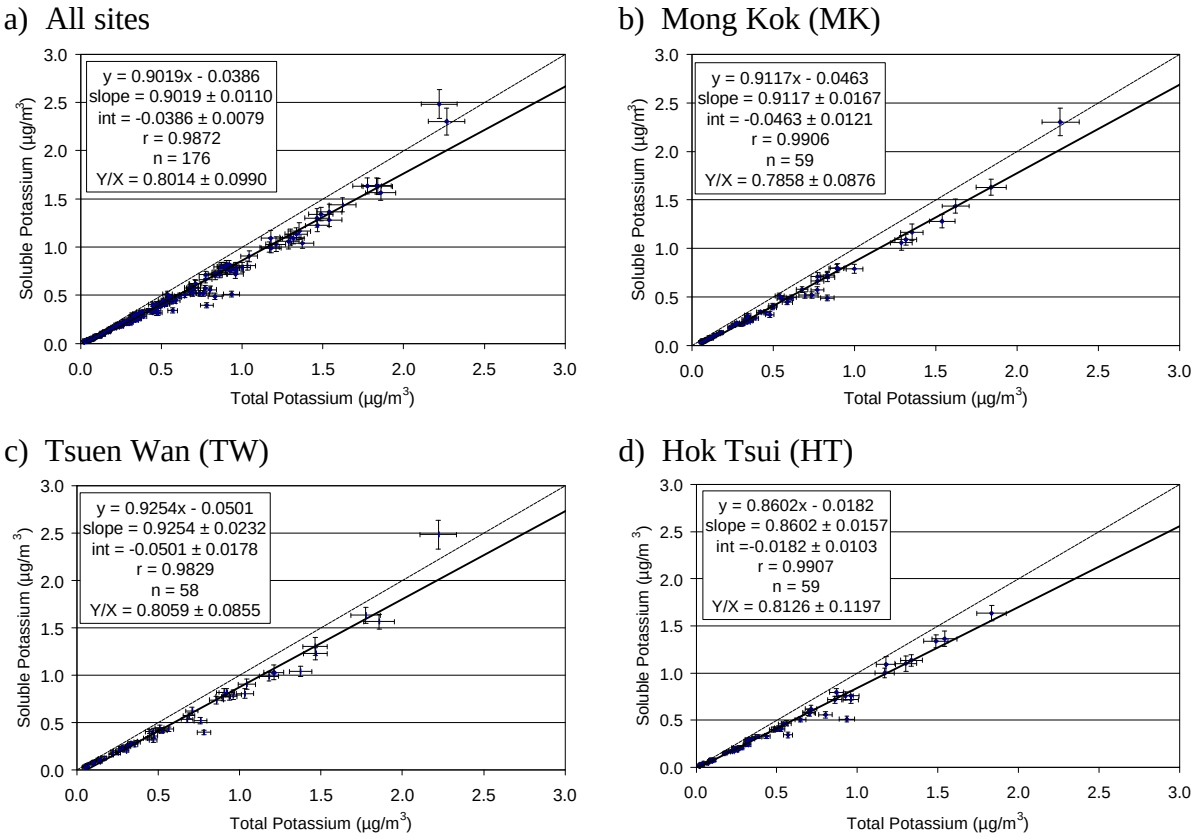

Figure 3-5. Scatter plots of soluble potassium versus total potassium measurements from $PM_{2.5}$ data acquired at: a) all three sites; b) the MK site; c) the TW site; and d) the HT site.

3.4.2.4 Ammonium Balance

Ammonium nitrate (NH_4NO_3), ammonium sulfate ($[NH_4]_2SO_4$), and ammonium bisulfate (NH_4HSO_4), are the most likely nitrate and sulfate compounds to be found in Hong Kong. Some sodium nitrate ($NaNO_3$) and/or sodium sulfate (Na_2SO_4) may also be present at the coastal sites, which may be attributable to transport by prevailing winds from the Pacific Ocean into Hong Kong, especially during summer. Ammonium (NH_4^+) can be calculated based on the stoichiometric ratios of the different compounds and compared with that which was measured. In Figure 3-6, ammonium is calculated from nitrate and sulfate, assuming that all nitrate was in the form of ammonium nitrate and all sulfate was in the form of either ammonium sulfate (i.e., calculated ammonium = [0.38 × sulfate] + [0.29 × nitrate]) or ammonium bisulfate (i.e., ammonium = [0.192 × sulfate] + [0.29 × nitrate]). These calculated values were compared with the measured values for ammonium.

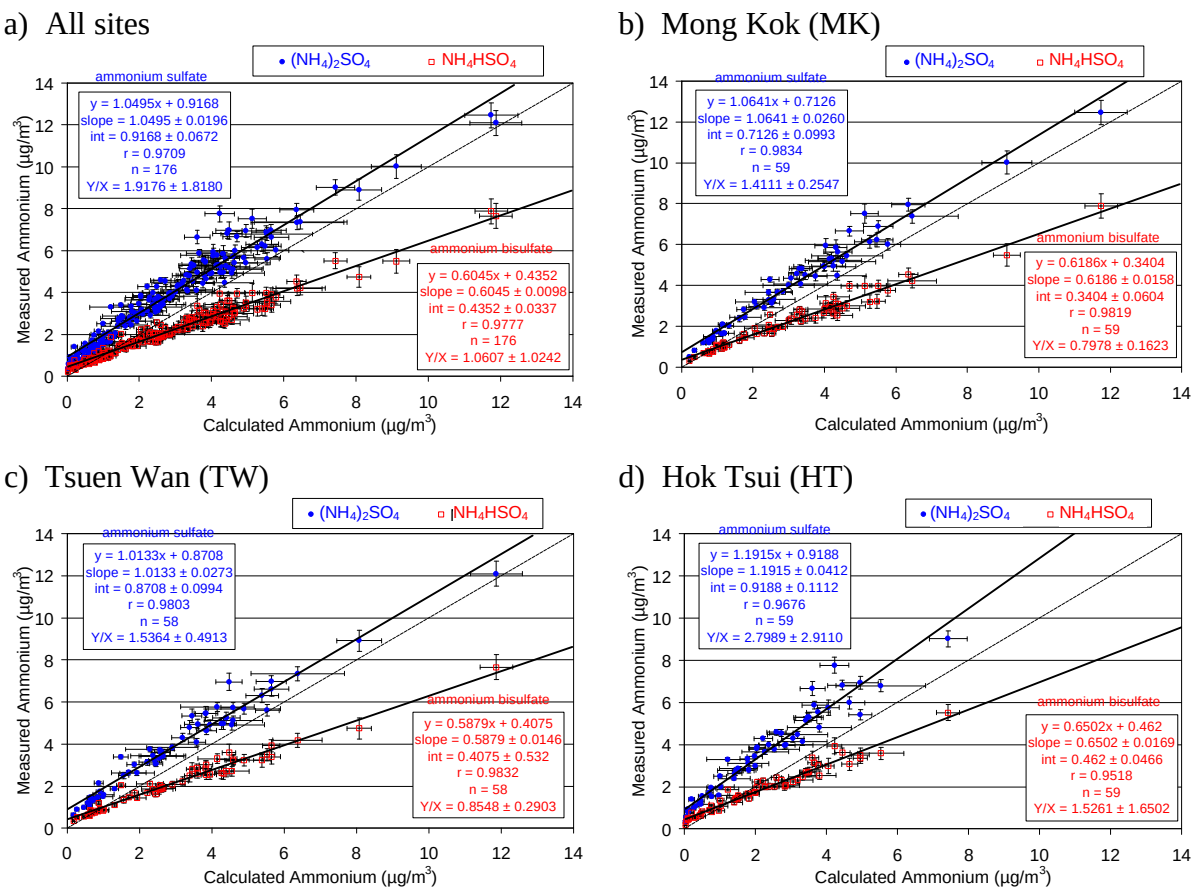

Figure 3-6. Scatter plots of calculated ammonium versus measured ammonium from $PM_{2.5}$ data acquired at: a) all three sites; b) the MK site; c) the TW site; and d) the HT site.

With a few exceptions during the study period, Figure 3-6 shows excellent agreement for $PM_{2.5}$ ammonium with a correlation coefficients exceeding 0.95 when ammonium sulfate or ammonium bisulfate was assumed. However, the slopes seen in these figures average 1.05±0.02 assuming ammonium sulfate, and 0.60±0.01 assuming ammonium bisulfate. These data thus imply that a majority of the sulfate was neutralized and in the form of ammonium sulfate during the study period. Based on the slopes from Figure 3-6, ammonium bisulfate may account for less than 12% of total sulfate.

When all sulfate and nitrate are assumed to be fully neutralized, calculated ammonium exceeds measured ammonium. This phenomenon typically is more pronounced in the PM_{10} fraction than in the $PM_{2.5}$ fraction, indicating the presence of coarse-particle sulfate and/or nitrate salts that might be associated with water-soluble Ca^{++} or Na^{+} ions. The chromatograms from ion chromatography analysis for nitrate and sulfate and graphs from automated colorimetry analysis for ammonium were examined, but no anomalies were found.

3.4.3 Anion and Cation Balance

The anion and cation balance in Figure 3-7 also shows a deficiency in cations that is not accounted for by measured anions. The correlations are high ($r>0.94$) in the $PM_{2.5}$ size fraction. The difference may be attributable to unmeasured H^+. The difference could also be due to the presence of coarse-particle sulfate and/or nitrate salts in a form other than ammonium sulfate and/or ammonium nitrate. However, Figure 3-7 generally indicates a close balance between anions and cations.

a) All sites

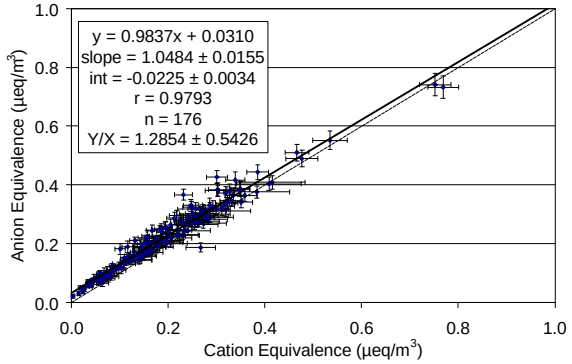

b) Mong Kok (MK)

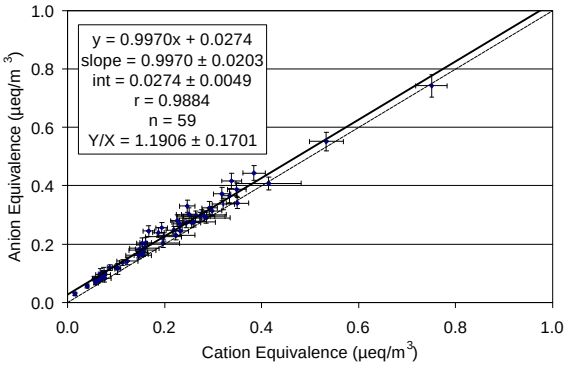

c) Tsuen Wan (TW)

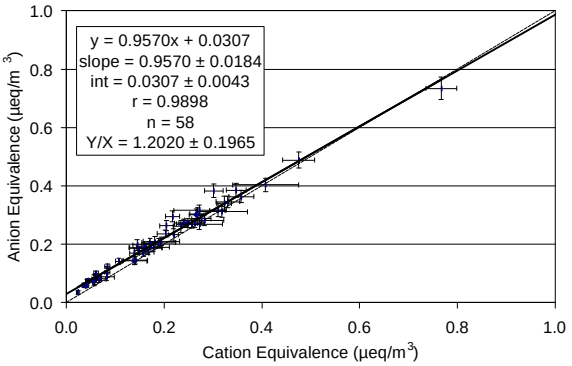

d) Hok Tsui (HT)

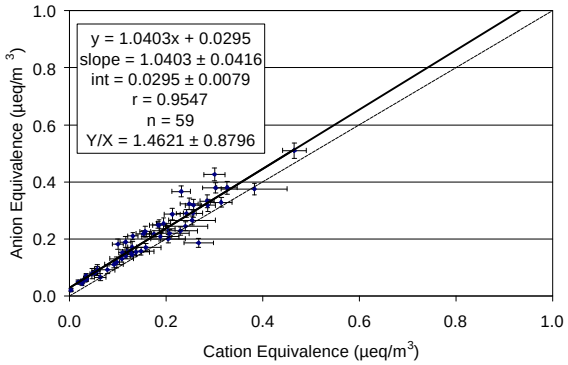

Figure 3-7. Scatter plots of cation versus anion measurements from $PM_{2.5}$ data acquired at: a) all three sites; b) the MK site; c) the TW site; and d) the HT site.

3.4.4 IMPROVE Protocol versus STN Protocol for Carbon Measurements

Total carbon (TC), OC, and EC determined by IMPROVE TOR and STN TOT methods for samples from each site and all sites combined are compared in Figure 3-8. STN TOT(i) and STN TOT(ii) represent two different ways of determining the OC/EC split, as described in Section 2.2. STN TOT(i) is the default protocol currently used in the USEPA Speciation Trends Network. In most of the cases, all three methods yield similar TC (<10% difference). Therefore, the mass fraction of carbonaceous material in $PM_{2.5}$ does not change when different methods are adopted. STN TOT(ii) EC can be significantly lower than IMPROVE EC because during the high temperature (900 °C) stage of the STN protocol, mineral oxides or carbonate on quartz filters may decompose and supply oxygen to neighboring carbon particles, resulting in the combustion of EC in a "pure He" environment (Chow et al., 2001).

At the TW and HT sites, IMPROVE TOR generally produced higher EC and lower OC than STN TOT(ii), and this agrees with the findings in Chow et al. (2001). STN TOT(i), which relies on optical correction for the OC/EC split, tends to yield results closer to IMPROVE TOR. At the MK site, ambient concentrations of EC and OC were much higher, and results from the IMPROVE and STN protocols are poorly correlated. The STN methods seem to overestimate EC when filters are heavily loaded. Overall, the adoption of different analytical protocols can yield significantly different OC and EC measurements, and this will influence the OC/EC partitioning in carbonaceous material.

a) All sites

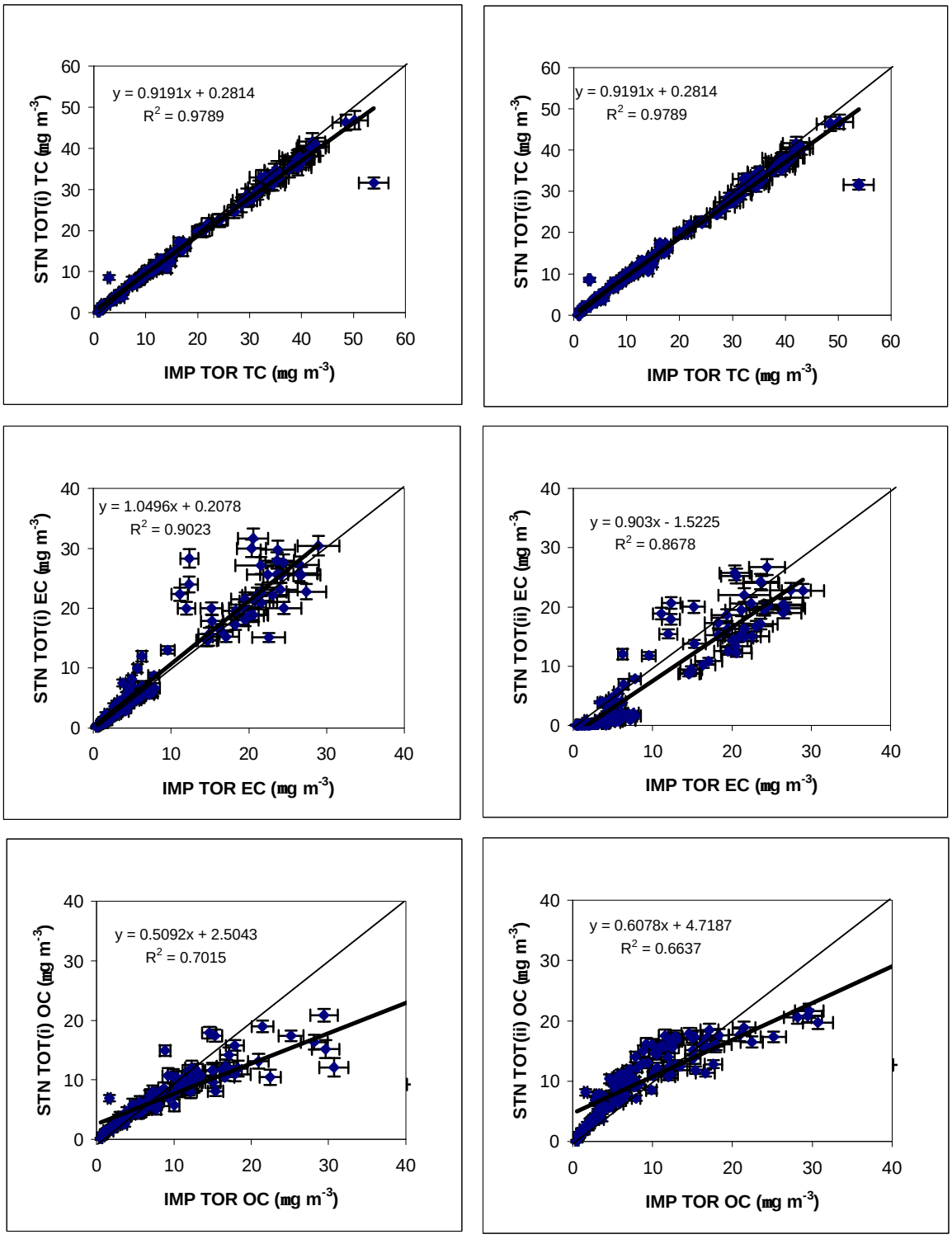

Figure 3-8. Comparisons of $PM_{2.5}$ with EC, OC, and EC determined by three different methods (one IMPROVE and two STN methods as defined in Section 2.2) at: a) all three sites, b) the MK site, c) the TW site, and d) the HT site.

b) Mong Kok (MK)

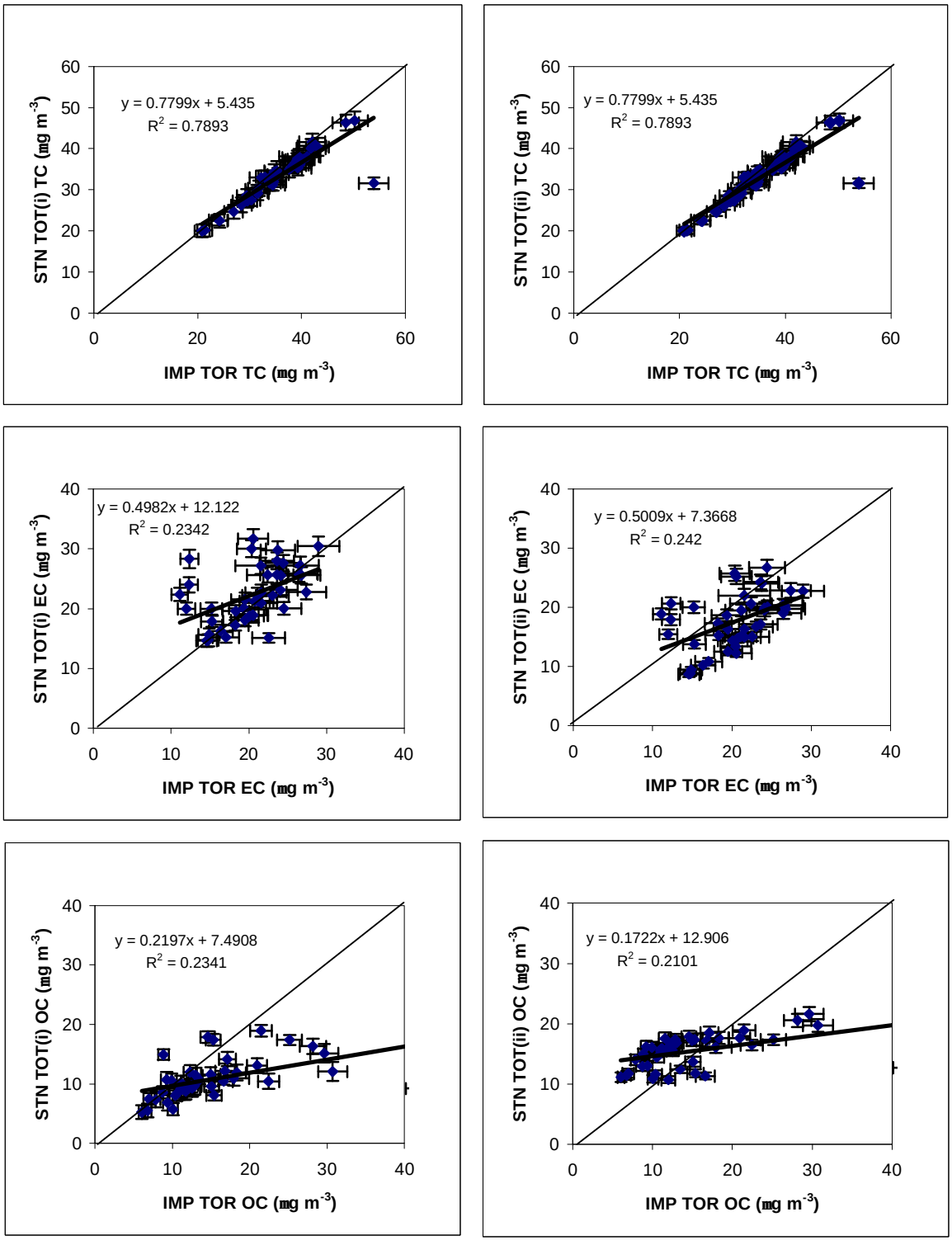

Figure 3-8. (continued)

c) Tsuen Wan (TW)

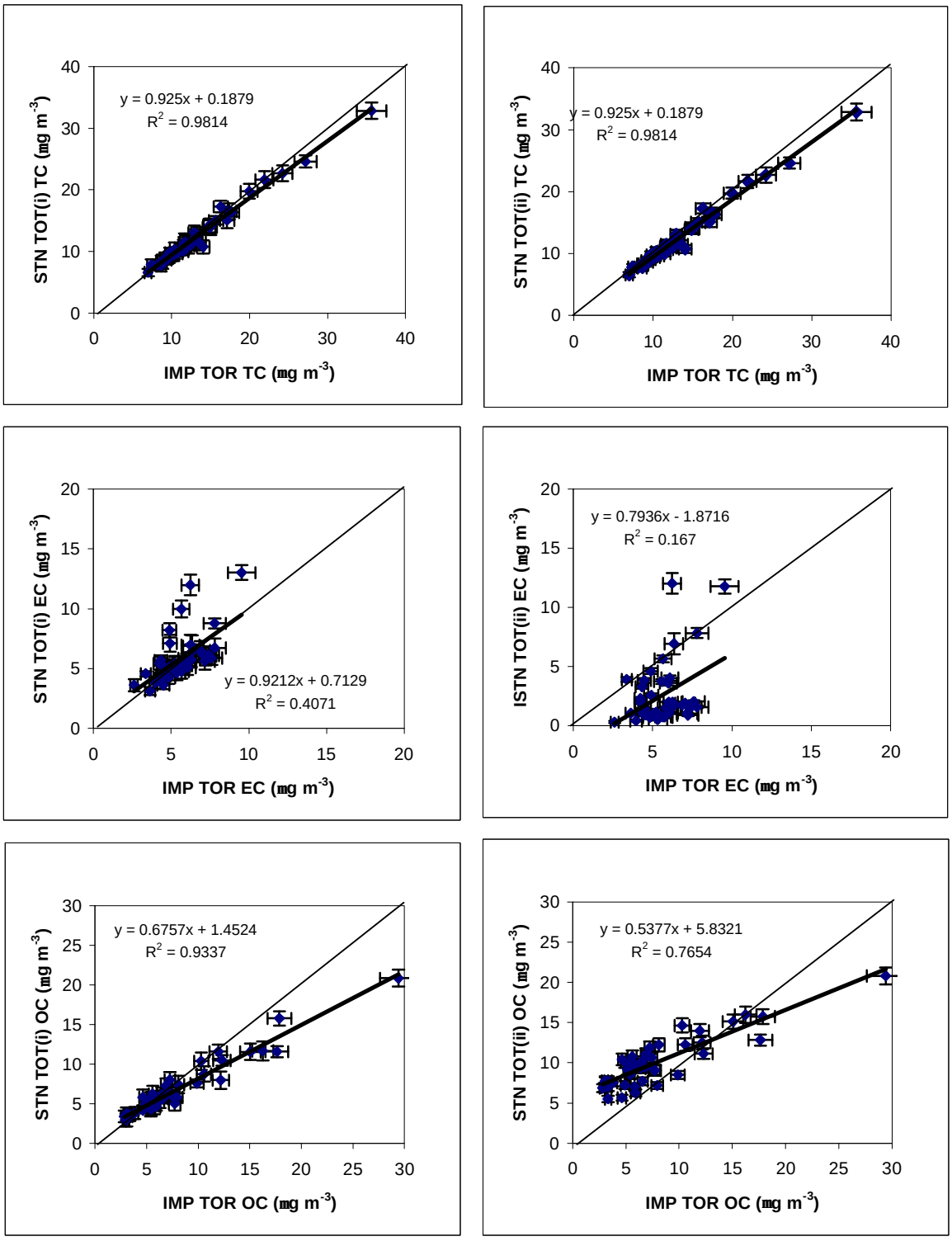

Figure 3-8. (continued)

d) Hok Tsui (HK)

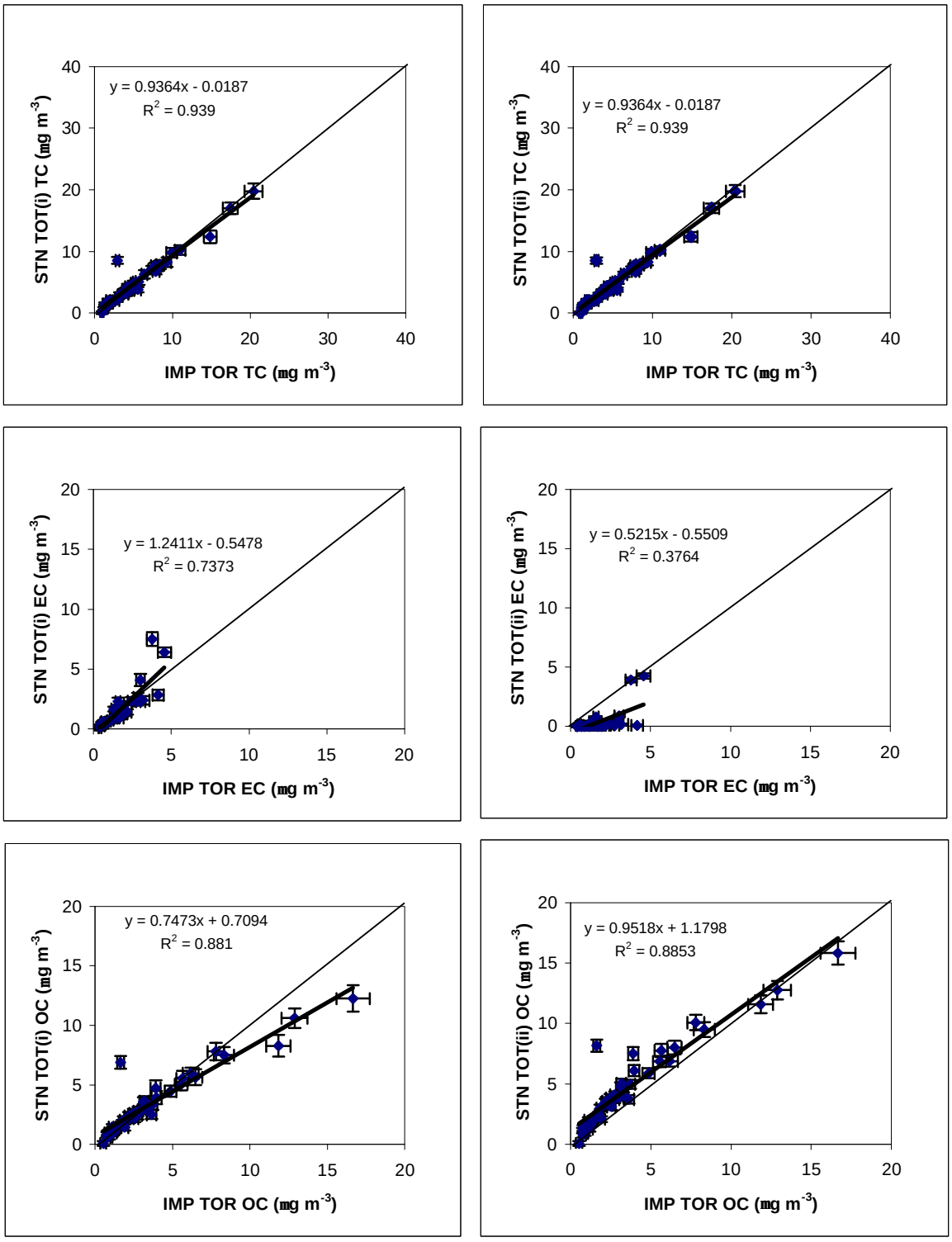

Figure 3-8. (continued)

3.4.5 Reconstructed versus Measured Mass

Major PM components can be used to reconstruct PM mass. The major components include: 1) geological material (estimated as 1.89×Al + 2.14×Si + 1.4×Ca + 1.43×Fe to account for unmeasured oxides), 2) organic matter (OM: 1.4×OC to account for unmeasured hydrogen and oxygen), 3) soot (elemental carbon), 4) ammonium sulfate, 5) ammonium nitrate, and 6) noncrustal trace elements (sum of other-than-geological trace elements). The difference between the constructed mass and the measured mass is referred to as unidentified mass.

The reconstructed mass are highly correlated to the measured mass at $r^2 \sim 0.98$ at all sites (Figure 3-9). In contrast to the sum-of-species-versus-mass comparison in Figure 3-2, unaccounted mass is largely eliminated when unmeasured oxygen and hydrogen were factored in. This confirms the validity of gravimetric and chemical measurements.

a) All sites

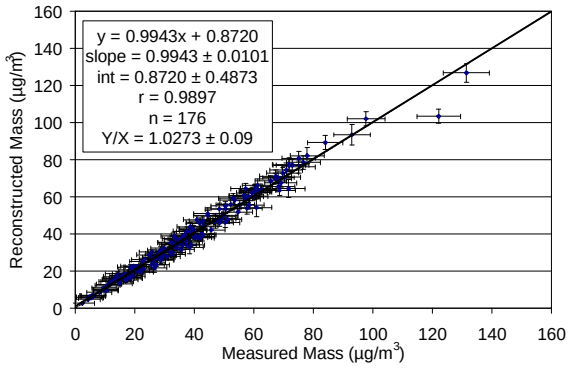

b) Mong Kok (MK)

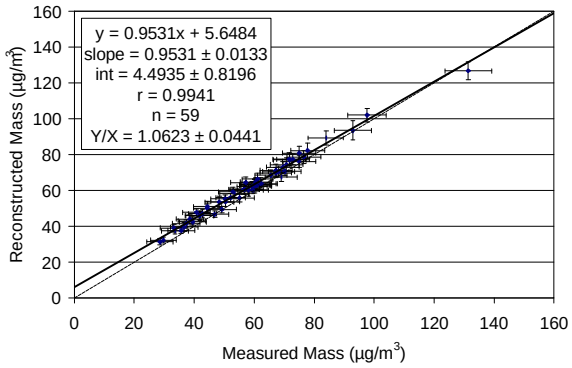

c) Tsuen Wan (TW)

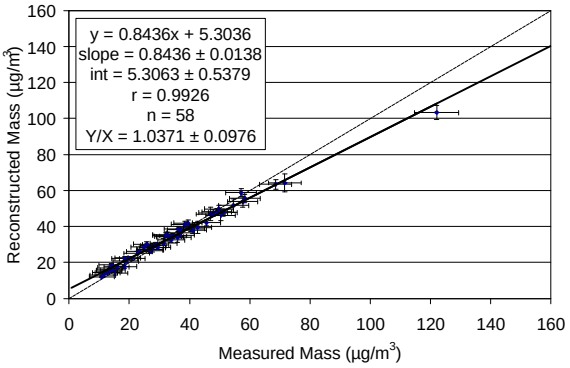

d) Hok Tsui (HT)

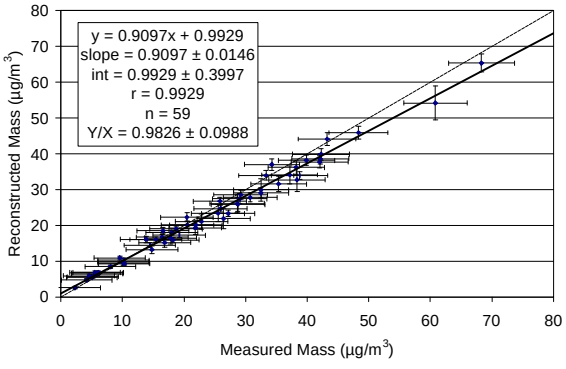

Figure 3-9. Scatter plots of reconstructed mass versus measured mass from $PM_{2.5}$ data acquired at: a) all three sites; b) the MK site; c) the TW site; and d) the HT site.

Figure 3-10 shows the annual average composition (%) of these major components to $PM_{2.5}$ mass. The unidentified mass was set to zero when the reconstructed mass is greater than the measured mass (i.e. unidentified mass is negative), and the mass fractions of the major components were adjusted accordingly. This occurred only at MK with unidentified mass ~ -3% of measured mass; this could be due to overestimation of some species, such as organic matter. At TW and HT, the unidentified mass was ~ 1% and ~ 7% of measured mass, respectively. To measure the gravimetric mass, Teflon filters were weighted at 30%-40% relative humidity. There could, however, still be residual water that accounted for the unidentified mass. Overall, the reconstructed mass agrees with the measured mass within ~ 10%.

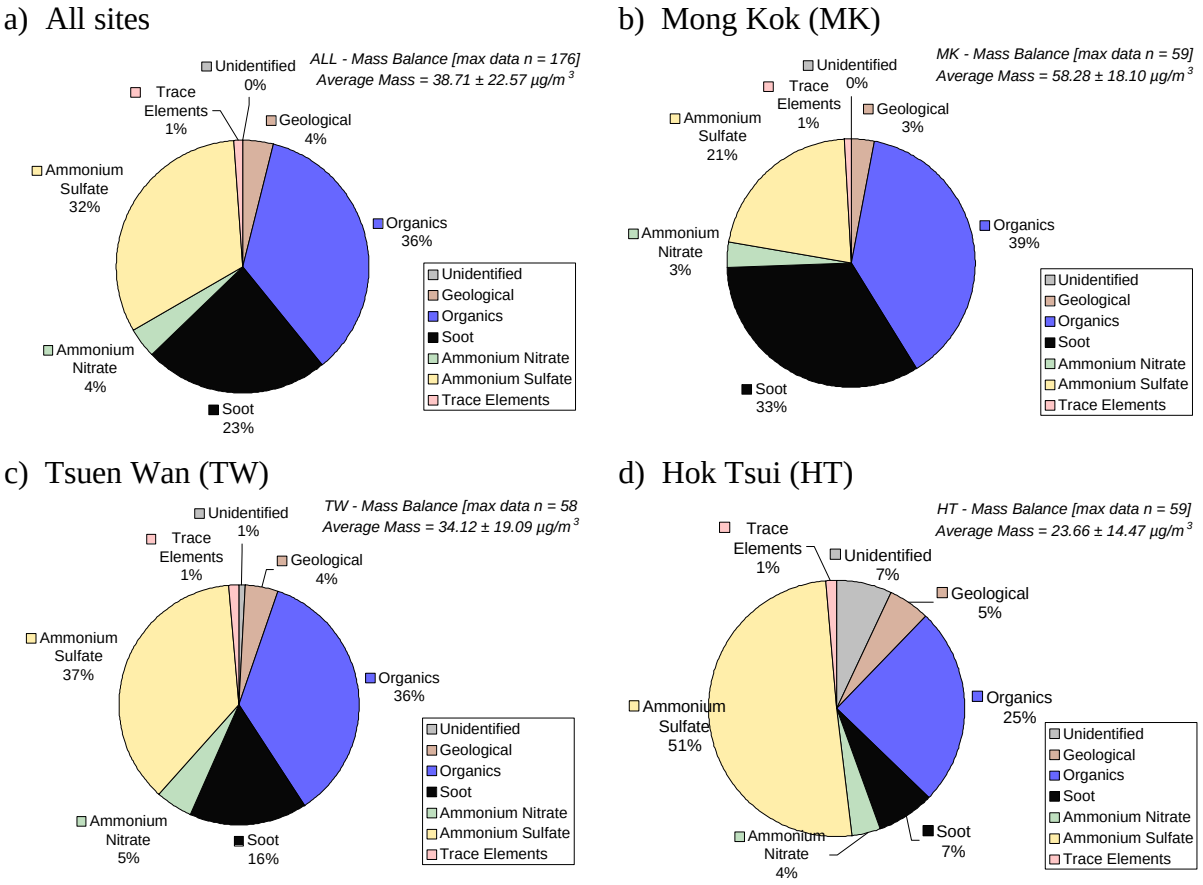

Figure 3-10. Material balance charts for $PM_{2.5}$ data acquired at: a) the three sites; b) the MK site; c) the TW site; and d) the HT site. The major components of reconstructed mass include: 1) geological material (estimated as 1.89×Al + 2.14×Si + 1.4×Ca + 1.43×Fe to account for unmeasured oxides), 2) organic matter (1.4×organic carbon to account for unmeasured hydrogen and oxygen), 3) soot (elemental carbon), 4) ammonium sulfate, 5) ammonium nitrate, 6) noncrustal trace elements (sum of other-than-geological elements listed in Table 3-4 excluding Al, Si, Ca, Fe, Cl, and S), and 7) unidentified mass (difference between measured mass and the sum of the major components).

Figure 3-11 demonstrates the average reconstructed mass for the highest and lowest 25% $PM_{2.5}$ days at the three sites. Nearby traffic emissions could be a relatively constant source of EC at the MK and TW sites. Although EC is an important part of mass at the MK and TW sites, EC concentrations vary little from low $PM_{2.5}$ days to high $PM_{2.5}$ days. The increased mass consists mostly of ammoniated sulfate and OM, both of which can be of secondary origin. Higher sulfate and OM are observed on high $PM_{2.5}$ days at all three sites, suggesting the presence of variable regional sources of sulfate and OM. The HT site does not have significant sources nearby, so most of the pollutants measured at this site were probably transported there from distant urban areas.

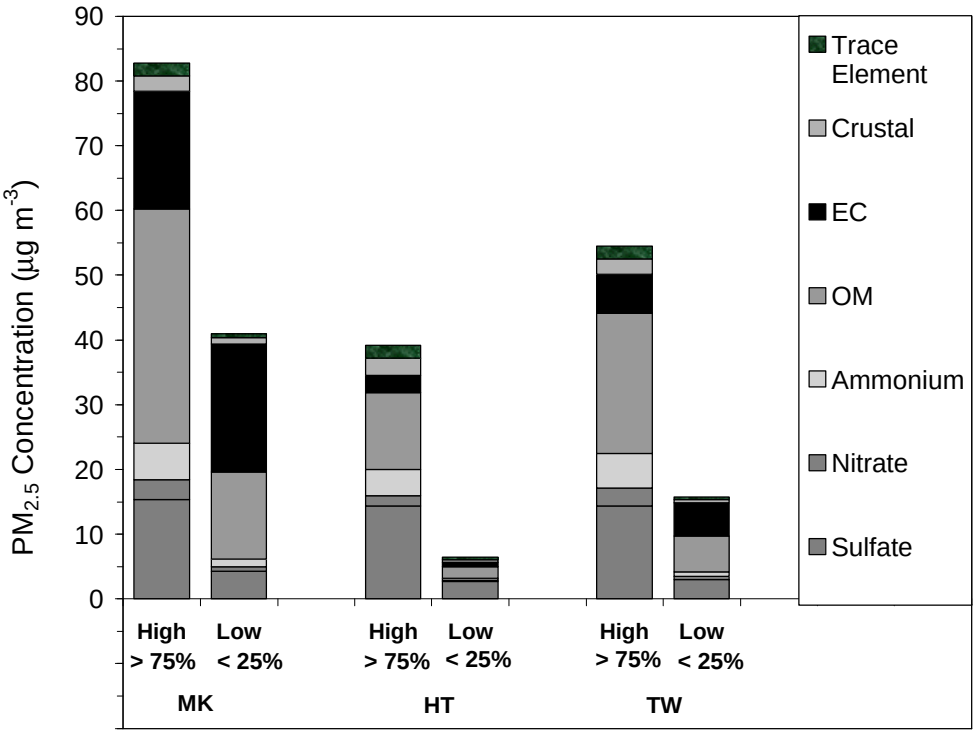

Figure 3-11. Mean reconstructed mass and chemical composition for highest and lowest 25% $PM_{2.5}$ days at the Mong Kok (MK), Hok Tsui (HT), and Tsuen Wan (TW) sites.

4. SUMMARY AND RECOMMENDATIONS

Between 11/6/2000 and 10/26/2001, chemically speciated $PM_{2.5}$ was measured every sixth day in Hong Kong at three sites representing air quality at roadside, urban, and rural areas. A total of 59 samples were collected from the Mong Kok (MK) and Tsuen Wan (TW) sites, and 58 from the Tsuen Wan (TW) site. The highest annual mean $PM_{2.5}$ mass of nearly 60 μg m^{-3} was found at the roadside MK site. The lowest annual mean of ~ 24 μg m^{-3} was found at the rural HT site, but this value is still much higher than the USEPA annual 24-hr $PM_{2.5}$ standard of 15 μg m^{-3}.

Data was validated through various comparisons between measurements. Reconstructed mass and measured mass were highly correlated with r^2 ~ 0.98, which further confirmed the validity of gravimetric and chemical measurements. Carbonaceous aerosol accounted for more than half of $PM_{2.5}$ mass at MK and TW, and was especially dominant at MK. The EC/OC ratio of almost 1 at the roadside MK site indicated the substantial influence of motor vehicle exhaust. Sulfate contributed nearly equally at all three sites, while nitrate was significantly lower at the rural HT site. Ammonium was well balanced by sulfate and nitrate at all three sites. Concentrations of crustal material and trace elements were low, accounting for < 10 % of $PM_{2.5}$ mass and lacking distinct spatial variations.

High sulfate concentrations did not necessarily appear in summer. The two highest sulfate episodes appeared on 2/28/01 and 9/14/01. Sulfate concentrations were similar at all three sites, suggesting that sulfate and its gaseous precursor (SO_2) may have originated from more distant upwind sources. Even though wind directions varied from winter to summer due to Asian monsoons, seasonal variations in sulfate concentrations were not clear. Measurements are needed over several years to establish a statistically significant seasonal variation.

EC concentrations at MK were significant higher than at HT and TW, but no significant seasonal trend was observed. OC at MK was generally higher in winter, which led to a lower EC/OC ratio in winter. Whether this is due to aerosol microphysics or atmospheric boundary layer dynamics warrants further investigation.

Crustal material concentrations at all three sites were also similar and may be attributable to long-range transport of fine-mode fugitive dust. A crustal episode occurred on 3/6/01 when northwesterly winds dominated. This episode could have been the tail of the Asian dust storm originating from the Gobi Desert.

Recommendations for future work include:

1. Long-term monitoring: The USEPA requires three years of monitoring to determine compliance with standards. This is to compensate for potential abnormalities in climate patterns that may significantly influence pollution levels. Long-term monitoring also helps to determine seasonal and interannual trends.

2. Source quantification: This study acquired rich inorganic and organic ambient data. However, better knowledge of local and regional pollution sources is needed in order to understand how emissions are related to ambient concentrations, human exposure, and health effects. Such knowledge can be obtained by measuring source emissions, determining emission profiles, and estimating emission inventories. Similar data from other countries are not necessarily applicable to Hong Kong because of differences in sources and atmospheric transformation.

3. Data analysis: A comprehensive data analysis effort that integrates meteorological and chemical data is very important to implementing effective pollution controls and regulations. This may include chemical mass balance analysis (which requires source information) and factor analysis to quantify contributions from all potential sources. Receptor models, such as wind rose and ensemble air parcel back trajectory, are useful for determining source regions and providing a basis for full chemical transport modeling.

5. REFERENCES

Bevington, P.R. (1969). *Data Reduction and Error Analysis for the Physical Sciences*. McGraw Hill, New York, NY.

Chow, J.C.; and Watson, J.G. (1989). Summary of particulate data bases for receptor modeling in the United States. In *Transactions, Receptor Models in Air Resources Management*, J.G. Watson, Ed. Air & Waste Management Association, Pittsburgh, PA, pp. 108-133.

Chow, J.C.; Watson, J.G.; Lowenthal, D.H.; Solomon, P.A.; Magliano, K.L.; Ziman, S.D.; and Richards, L.W. (1993a). PM_{10} and $PM_{2.5}$ compositions in California's San Joaquin Valley. *Aerosol Sci. Technol.,* **18**:105-128.

Chow, J.C.; Watson, J.G.; Pritchett, L.C.; Pierson, W.R.; Frazier, C.A.; and Purcell, R.G. (1993b). The DRI Thermal/Optical Reflectance carbon analysis system: Description, evaluation and applications in U.S. air quality studies. *Atmos. Environ.,* **27A**(8):1185-1201.

Chow, J.C.; Fujita, E.M.; Watson, J.G.; Lu, Z.; Lawson, D.R.; and Ashbaugh, L.L. (1994). Evaluation of filter-based aerosol measurements during the 1987 Southern California Air Quality Study. *Environmental Monitoring and Assessment,* **30**:49-80.

Chow, J.C.; and Watson, J.G. (1994). Guidelines for PM_{10} sampling and analysis applicable to receptor modeling. Report No. EPA-452/R-94-009. Prepared for U.S. EPA, Office of Air Quality Planning and Standards, Research Triangle Park, NC, by Desert Research Institute, Reno, NV.

Chow, J.C. (1995). Critical review – Measurement methods to determine compliance with ambient air quality standards for suspended particles. *J. Air & Waste Manage. Assoc.,* **45**(5):320-382.

Chow, J.C.; Watson, J.G.; Lu, Z.; Lowenthal, D.H.; Frazier, C.A.; Solomon, P.A.; Thuillier, R.H.; and Magliano, K.L. (1996). Descriptive analysis of $PM_{2.5}$ at regionally representative locations during SJVAQS/AUSPEX. *Atmos. Environ.,* **30**(12):2079-2112.

Chow, J.C.; and Watson, J.G. (1999). Ion chromatography in elemental analysis. In *Elemental Analysis of Airborne Particles, Vol. 1,* S. Landsberger and M. Creatchman, Eds. Gordon and Breach Science, Amsterdam, pp. 97-137.

Chow, J.C.; Watson, J.G.; Crow, D.; Lowenthal, D.H.; and Merrifield, T. (2001). Comparison of IMPROVE and NIOSH carbon measurements. *Aerosol Sci. Technol.,* **34**(1):23-34.

Fitz, D.R. (1990). Reduction of the positive organic artifact on quartz filters. *Aerosol Sci. Technol.,* **12**(1):142-148.

Green, M.C.; Chow, J.C.; Hecobian, A.; Etyemezian, V.; Kuhns, H.; and Watson, J.G. (2002). Las Vegas Valley Visibility and $PM_{2.5}$ Study. Final report. Prepared for Clark County Department of Air Quality Management, Las Vegas, NV, by Desert Research Institute, Las Vegas, NV. 6 May 2002.

Hidy, G.M. (1985). Jekyll Island meeting report: George Hidy reports on the acquisition of reliable atmospheric data. *Environ. Sci. Technol.,* **19**(11):1032-1033.

Lee, K.W.; and Ramamurthi, M. (1993). Filter collection. In *Aerosol Measurement: Principles, Techniques and Applications*, K. Willeke and P.A. Baron, Eds. Van Nostrand, Reinhold, New York, NY, pp. 179-205.

Lioy, P.J.; Watson, J.G.; and Spengler, J.D. (1980). APCA specialty conference workshop on baseline data for inhalable particulate matter. *JAPCA,* **30**(10):1126-1130.

Lippmann, M. (1989). Sampling aerosols by filtration. In *Air Sampling Instruments for Evaluation of Atmospheric Contaminants*, 7 ed., S.V. Hering, Ed. American Conference of Governmental Industrial Hygienists, Cincinnati, OH, pp. 305-336.

NIOSH (1996). Method 5040 Issue 1 (Interim): Elemental carbon (diesel exhaust). In *NIOSH Manual of Analytical Methods,* 4th ed. National Institute of Occupational Safety and Health, Cincinnati, OH.

NIOSH (1998). Method 5040 Issue 2 (Interim): Elemental carbon (diesel exhaust). In *NIOSH Manual of Analytical Methods,* 4th ed. National Institute of Occupational Safety and Health, Cincinnati, OH.

NIOSH (1999). Method 5040 Issue 3 (Interim): Elemental carbon (diesel exhaust). In *NIOSH Manual of Analytical Methods,* 4th ed. National Institute of Occupational Safety and Health, Cincinnati, OH.

Turpin, B.J.; Huntzicker, J.J.; and Hering, S.V. (1994). Investigation of organic aerosol sampling artifacts in the Los Angeles Basin. *Atmos. Environ.,* **28**(19):3061-3071.

Watson, J.G.; Chow, J.C.; Richards, L.W.; Andersen, S.R.; Houck, J.E.; and Dietrich, D.L. (1988). The 1987-88 Metro Denver Brown Cloud Air Pollution Study, Volume II: Measurements. Report No. 8810.1F2. Prepared for 1987-88 Metro Denver Brown Cloud Study, Inc.; Greater Denver Chamber of Commerce, Denver, CO, by Desert Research Institute, Reno, NV.

Watson, J.G.; Lioy, P.J.; and Mueller, P.K. (1989). The measurement process: Precision, accuracy, and validity. In *Air Sampling Instruments for Evaluation of Atmospheric Contaminants*, 7th ed., S.V. Hering, Ed. American Conference of Governmental Industrial Hygienists, Cincinnati, OH, pp. 51-57.

Watson, J.G.; and Chow, J.C. (1992). Data bases for PM_{10} and $PM_{2.5}$ chemical compositions and source profiles. In *PM_{10} Standards and Nontraditional Particulate Source Controls*, J.C. Chow and D.M. Ono, Eds. Air & Waste Management Association, Pittsburgh, PA, pp. 61-91.

Watson, J.G.; and Chow, J.C. (1993). Ambient air sampling. In *Aerosol Measurement: Principles, Techniques and Applications*, K. Willeke and P.A. Baron, Eds. Van Nostrand, Reinhold, New York, NY, pp. 622-639.

Watson, J.G.; and Chow, J.C. (1994). Particle and gas measurements on filters. In *Environmental Sampling for Trace Analysis*, B. Markert, Ed. VCH, New York, pp. 125-161.

Watson, J.G.; Chow, J.C.; Lowenthal, D.H.; Pritchett, L.C.; Frazier, C.A.; Neuroth, G.R.; and Robbins, R. (1994). Differences in the carbon composition of source profiles for diesel- and gasoline-powered vehicles. *Atmos. Environ.*, **28**(15):2493-2505.

Watson, J.G.; Chow, J.C.; and Frazier, C.A. (1999). X-ray fluorescence analysis of ambient air samples. In *Elemental Analysis of Airborne Particles, Vol. 1*, S. Landsberger and M. Creatchman, Eds. Gordon and Breach Science, Amsterdam, pp. 67-96.

Watson, J.G.; Turpin, B.J.; and Chow, J.C. (2001). The measurement process: Precision, accuracy, and validity. In *Air Sampling Instruments for Evaluation of Atmospheric Contaminants*, 9th ed., B.S. Cohen and C.S.J. McCammon, Eds. American Conference of Governmental Industrial Hygienists, Cincinnati, OH, pp. 201-216.